NASA CONTRACTOR REPORT

NASA CR-1946

TIME AND TEMPERATURE DEPENDENT MODULUS OF PYRRONE AND POLYIMIDE MOLDINGS

by L. L. Lander

Prepared by
AVCO SYSTEMS DIVISION
Lowell, Mass. 01851
for Langley Research Center

NATIONAL AERONAUTICS AND SPACE ADMINISTRATION • WASHINGTON, D. C. • JANUARY 1972

1. Report No.	2. Government Accession No.	3. Recipient's Catalog No.
NASA CR-1946		

4. Title and Subtitle	5. Report Date
TIME AND TEMPERATURE DEPENDENT MODULUS OF PYRRONE & POLYIMIDE MOLDINGS	January 1972
	6. Performing Organization Code
7. Author(s) L. L. Lander	8. Performing Organization Report No.
	10. Work Unit No.
9. Performing Organization Name and Address AVCO Corporation Systems Division Lowell, Massachusetts 01851	11. Contract or Grant No. NAS1-8495
	13. Type of Report and Period Covered Contractor Report
12. Sponsoring Agency Name and Address National Aeronautics & Space Administration Washington, D.C. 20546	14. Sponsoring Agency Code

15. Supplementary Notes

16. Abstract A method is presented by which the modulus obtained from a stress relaxation test can be used to estimate the modulus which would be obtained from a sonic vibration test. The method was applied to stress relaxation, sonic vibration, and high speed stress-strain data which was obtained on a flexible epoxy. The modulus as measured by the three test methods was identical for identical test times, and a change of test temperature was equivalent to a shift in the logarithmic time scale. An estimate was then made of the dynamic modulus of moldings of two Pyrrones and two polyimides, using stress relaxation data and the method of analysis which was developed for the epoxy. Over the common temperature range (350° to 500°K) in which data from both types of tests were available, the estimated dynamic modulus value differed by only a few percent from the measured value. As a result, it is concluded that, over the 500° to 700°K temperature range, the estimated dynamic modulus values are accurate.

17. Key Words (Suggested by Author(s))	18. Distribution Statement
Epoxy Dynamic modulus Polyimide Mechanical damping Pyrrone Stress relaxation Time-temperature superposition	Unclassified - Unlimited

19. Security Classif. (of this report)	20. Security Classif. (of this page)	21. No. of Pages	22. Price*
Unclassified	Unclassified	78	$ 3.00

*For sale by the National Technical Information Service, Springfield, Virginia 22151

FOREWORD

This report was prepared by AVCO Corporation, Systems Division, Lowell, Massachusetts 01851, under National Aeronautics and Space Administration Contract NAS1-8495 titled, "Investigation of Dynamic Mechanical Properties of Pyrrone and Modified Polyimide Moldings." This program was administered under the direction of the Langley Research Center, Hampton, Virginia 23365. The Author, Mr. L. L. Lander of the Mechanical Evaluation Group, served as Program Manager.

Messers C. Theberge and D. Dowell of AVCO performed the experimental work, and Mr. P. Roy performed the analytical studies associated with the development of the dynamic modulus apparatus.

TABLE OF CONTENTS

LIST OF TABLES

LIST OF FIGURES

LIST OF FIGURES (concl'd)

TIME AND TEMPERATURE DEPENDENT MODULUS OF PYRRONE AND POLYIMIDE MOLDINGS

By L. L. Lander
AVCO Systems Division

INTRODUCTION

In a program to measure the dynamic modulus of polymer moldings by sonic vibrations, the temperature range of interest was 100° to 700°K. However, for experimental reasons, it was possible to obtain the dynamic modulus over a shorter range of 100° to 500°K. An alternate method of stress relaxation was used to measure the modulus over the range of 350° to 700°K. Consequently it was necessary to show that (1) the stress relaxation modulus could be made to yield an equivalent dynamic modulus in the common temperature range (350° to 500°K) and (2) the stress relaxation modulus could then be used to estimate the dynamic modulus in the experimentally inaccessible temperature range (500° to 700°K).

The purpose of this report is to show how the stress relaxation modulus data can be analyzed to provide an estimate of the dynamic modulus over a wide temperature range.

SYMBOLS

E^*	Dynamic modulus, psi
e_{ij}	Deviatoric strain tensor
f	Frequency, Hz
G_1	Deviatoric relaxation function
G_2	Volumetric relaxation function
K	Constant, 9.128 for rectangular specimens, 11.268 for cylindrical specimens
L	Specimen length, inches
M	Specimen mass, grams
Q	Specimen shape factor, width times thickness for rectangular specimens, diameter squared for cylindrical specimens
s_{ij}	Deviatoric stress tensor
T	Temperature, ^{o}K
t	Time
Δ	Damping factor
δ_{ij}	Kronecker delta
ϵ_{ij}	Volumetric strain tensor
ϕ	Temperature shift function
σ_{ij}	Volumetric stress tensor
τ	Time, seconds

MATERIALS AND TESTS

Materials

Moldings of four polymers, two Pyrrones and two polyimides, were used in this investigation. One Pyrrone, an oligomer type designated Pyrrone A, was synthesized from benzophenone tetracarboxylic acid dianhydride (BTDA) and diaminobenzidine (DAB). Details of the synthesis and molding are given in reference 1. A second Pyrrone, a salt-like intermediate designated Pyrrone L, was synthesized and molded from the same monomers (BTDA and DAB) as described in references 2 and 3. The two polyimides were both available commercially, and details of the synthesis and molding of these polymers are not generally available. However, one polyimide, designated polyimide B, is thought to be synthesized from BTDA and meta phenylenediamine (mPDA). The other polyimide, designated polyimide P, is thought to be synthesized from pyromellitic dianhydride (PMDA) and oxydianiline (ODA).

Although most of the polymer moldings had no reinforcing agents or additives, one group of Pyrrone A contained 15 weight percent graphite. Some of the moldings had received either thermal aging or electron irradiation before testing. Since such treatment had no significant effect on the time-temperature analysis in this report, only average values of modulus and damping are reported and no distinction is made as to the pre-test treatment.

Tests

Three types of thermomechanical tests were performed and the details are given in Appendix A. The dynamic modulus and damping factor were determined in the temperature range of 100° to 500°K. The technique used was that of a fixed-free resonating beam. Compressive stress relaxation tests to 10^2 seconds were performed over the range from 350° to 700°K with one series extending from 160° to 700°K. The thermal expansion was measured with quartz tube dilatometers over the range of 100° to 500°K.

TIME-TEMPERATURE EQUIVALENCE

The constitutive equations for a linear homogeneous, isotropic, viscoelastic solid can be cited in integral form (ref. 4) as:

$$S_{ij}(x,\tau) = \int_{-\infty}^{\tau} G_1(\tau-\tau') \frac{\partial}{\partial\tau'} e_{ij}(x,\tau)\,d\tau' \tag{1}$$

$$\sigma_{kk}(x,\tau) = \int_{-\infty}^{\tau} G_2(\tau-\tau') \frac{\partial}{\partial\tau'} \epsilon_{kk}(x,\tau)\,d\tau' \tag{2}$$

where $G_1(\tau)$ is the deviatoric relacation function and $G_2(\tau)$ is the volumetric relaxation function at uniform temperature and s_{ij} and e_{ij} are deviatoric stress and strain tensors. In other words, the behavior of a viscoelastic material can be considered a function of time and strain only, with no need to incorporate a strain rate term. This fact can be demonstrated as follows.

Effect of Time

First, consider the type of data obtained in a stress relaxation experiment in which a specimen is maintained at some predetermined strain level and the stress required to maintain this strain is recorded as a function of time. The data presented in Figure 1 are an example. This is a double logarithm (or log-log) plot of stress versus time obtained on a flexible epoxy (ref. 5). Samples were compressed at room temperature to a strain of .005 in./in. in 10^{-3} seconds and the stress as a function of time was recorded out to 10^{+2} seconds. Dividing the stress at any time (τ) by the strain (.005 in./in.) would give the data for a time-dependent modulus as shown in Figure 2.

By contrast, in high strain rate tensile or compressive tests both the stress and strain are recorded as a function of time as shown in Figure 3. These data are then cross plotted to obtain a stress-strain curve as shown in Figure 4, from which the conventional engineering parameters of modulus, strength, and total strain are determined. When presenting these data it is conventional to plot them as a function of strain rate (the slope of the strain-time curve of Figure 3). For example, the room temperature tensile and compressive modulus of a flexible epoxy, obtained from high strain rate tests, are shown in Figure 5.

There are now two characteristic moduli, one expressed as a function time (τ), the other expressed as a function of strain rate ($\dot{\epsilon}$). According to reference 6 these data should be comparable on the basis of time.

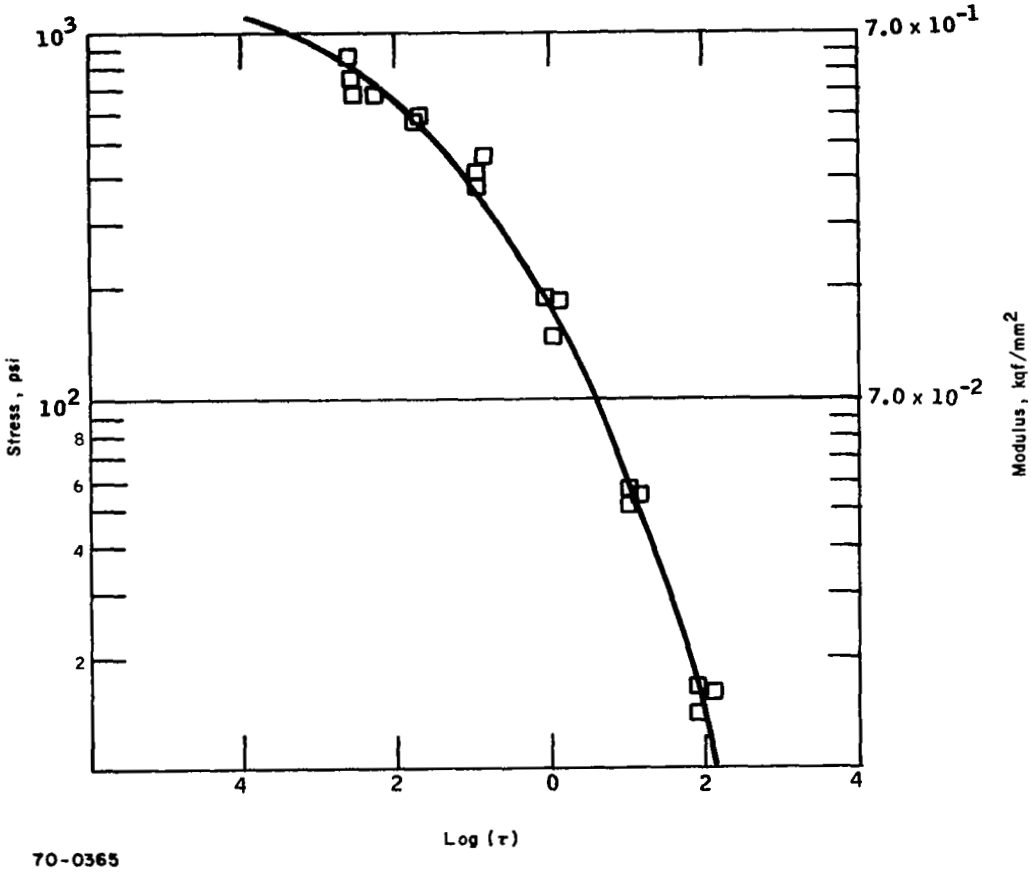

Figure 1 STRESS VERSUS TIME

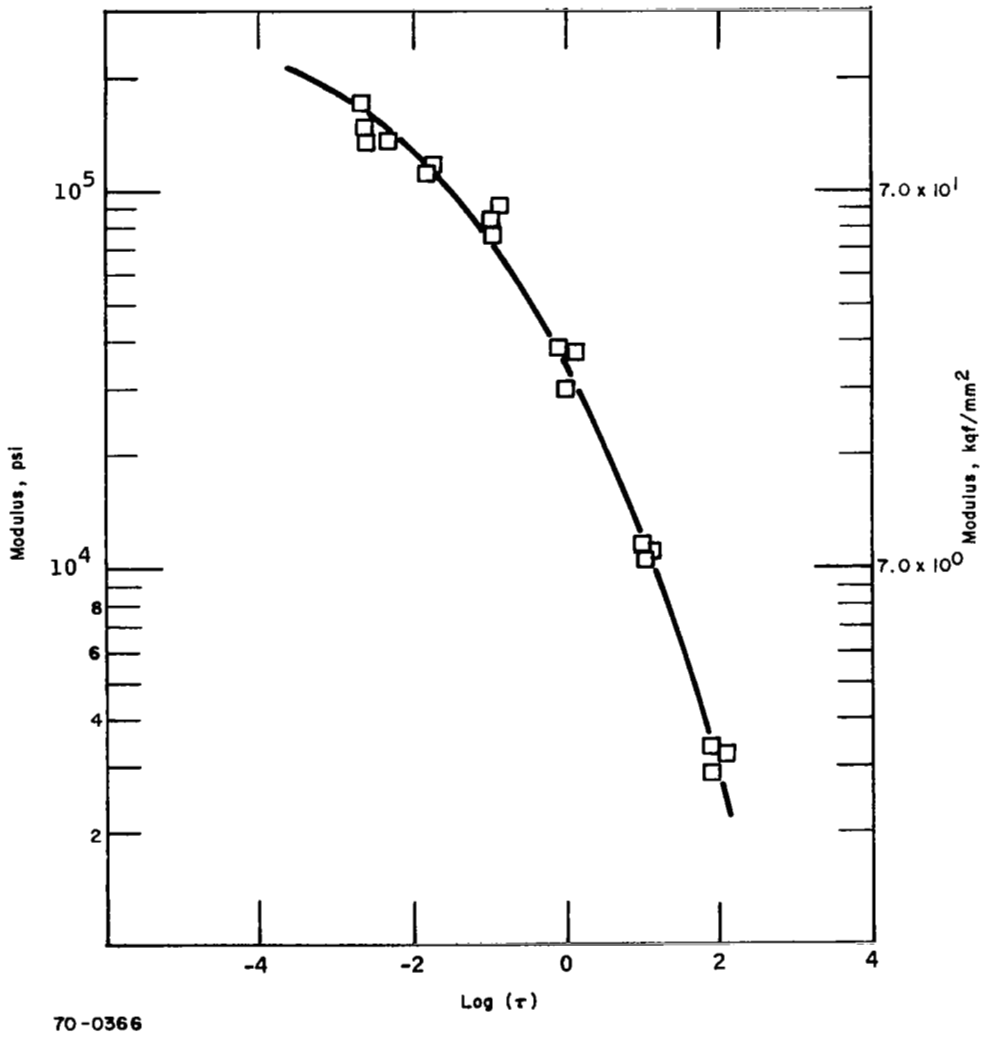

Figure 2 RELAXATION MODULUS VERSUS TIME

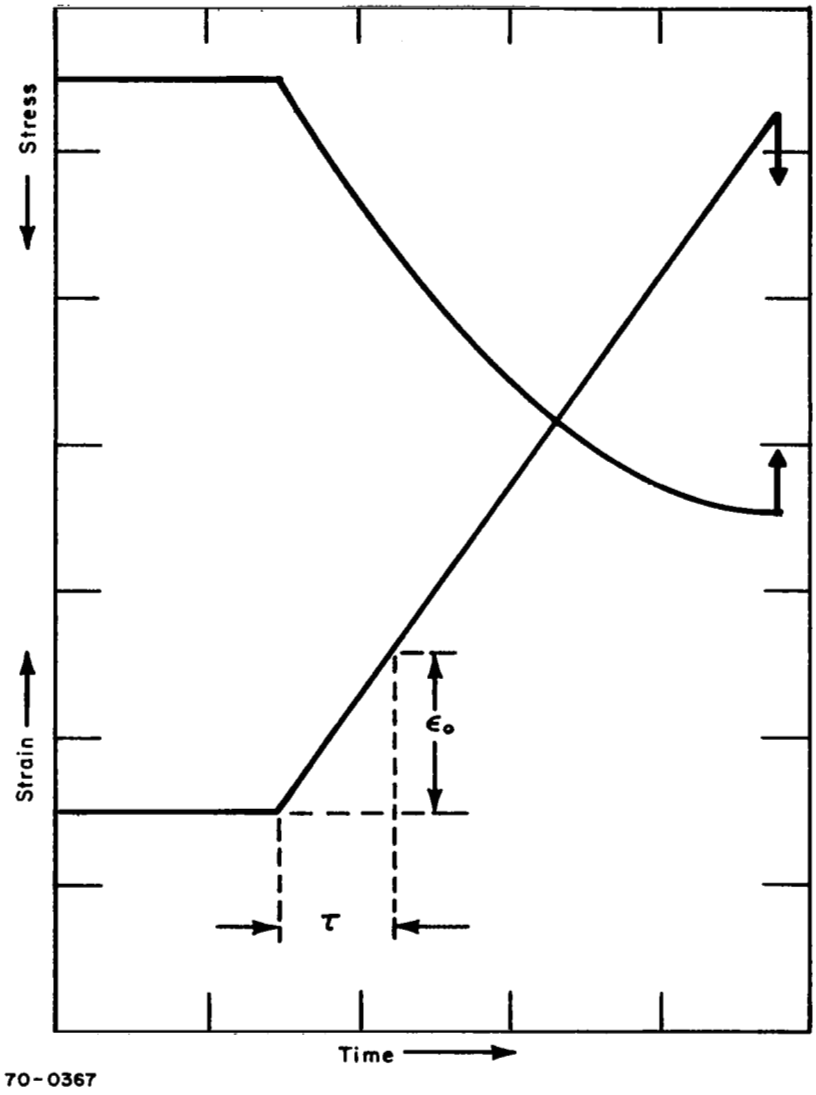

Figure 3 TYPICAL STRESS-TIME, STRAIN-TIME RECORD

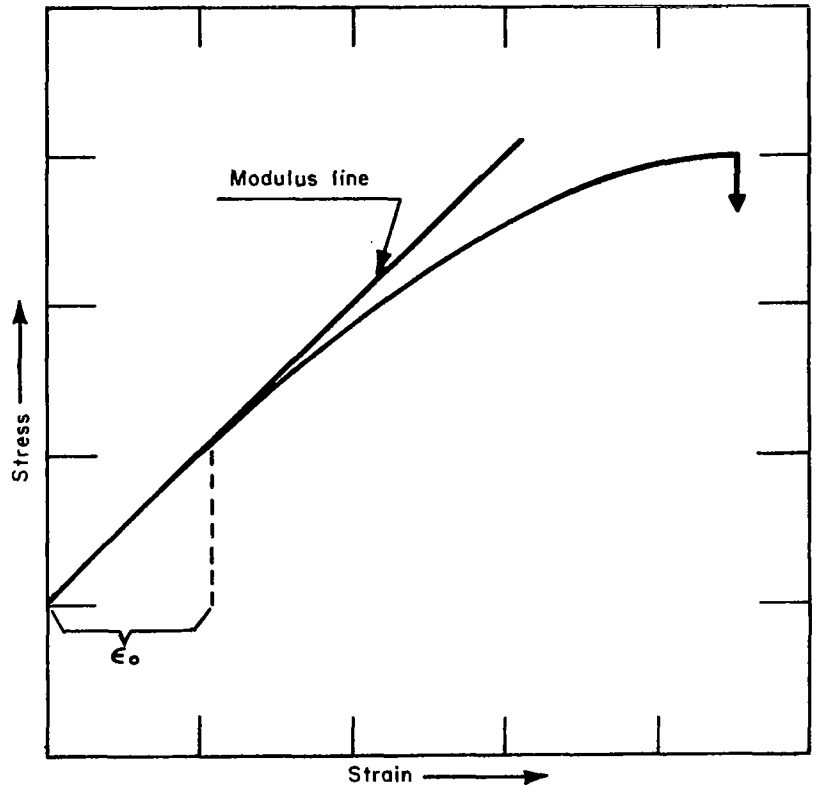

70-0368

Figure 4 TYPICAL STRESS-STRAIN CURVE

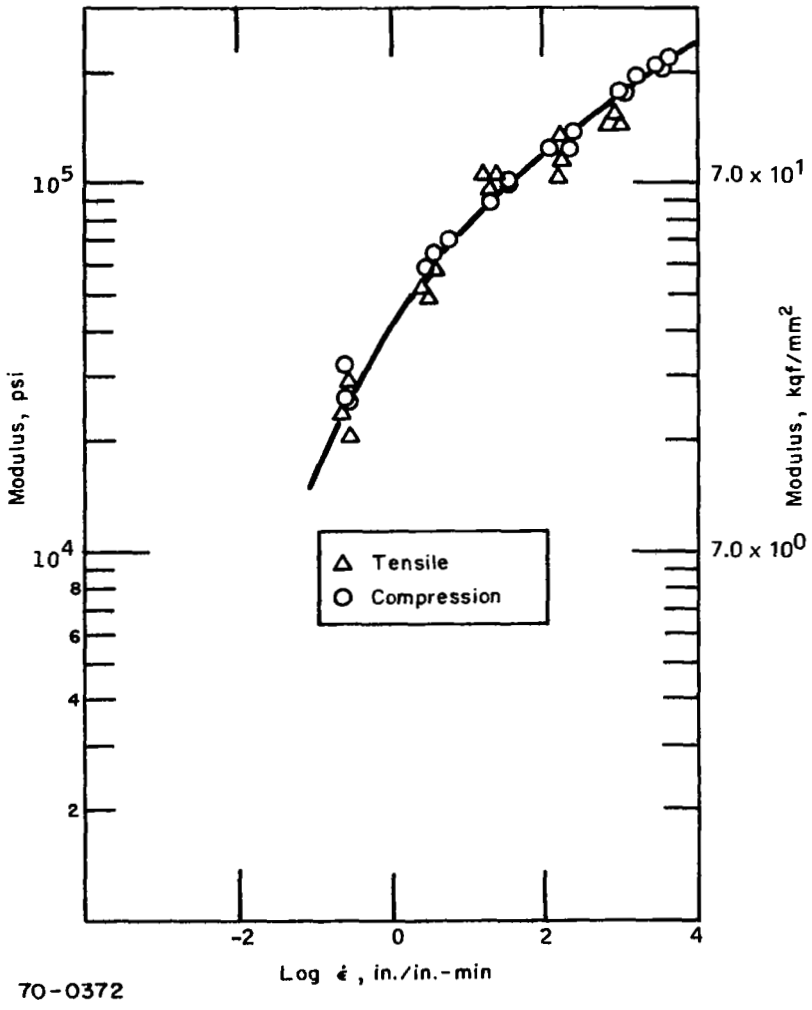

Figure 5 MODULUS VERSUS STRAIN RATE

It is assumed that the results of all deformations and loadings that the specimen has undergone prior to the experiment have completely disappeared or can be considered negligible (ref. 4). This implies that the integral from $t = -\infty$ to $t = \tau_0$ (τ_0 being the beginning of the experiment) is essentially equal to zero and that the time scale of interest is then from $t = \tau_0$ to $t = \tau$, the duration of the experiment. To determine the duration of the experiment it is necessary to determine the strain (ϵ_0) at which the modulus was measured (Figure 4). The duration of the test (τ) is the time required to reach the strain ϵ_0 (Figure 3). With the test duration so determined, it is possible to plot modulus (as measured in high strain rate tensile and compressive tests) versus time and compare these data with those measured in the relaxation tests. The moduli are compared in Figure 6 where it is seen that when time is considered the independent variable, the data from these two types of experiments take on the same values.

As an extension of this argument consider a double cantilever beam, clamped in the center as shown in Figure 7, and excited into resonance. Under these conditions, the strain rate is constant only along the neutral axis and the ends and is equal to zero. At all other points in the beam, the strain rate varies from zero to some finite maximum at the outer fiber at the center of the beam. A flexible epoxy beam with the dimensions of 10 x 1 x .75 inches and a density of 1.19 gm/cm^3 was found to resonate at 147 Hz. This corresponds to a modulus of 1.8×10^5 psi. In this instance, the duration of the experiment is the time required to go from zero to maximum strain; or one-fourth the period of oscillation. With a resonant frequency of 147 Hz the duration of the experiment is 1.7×10^{-3} second. From Figure 6 it is seen that the dynamic modulus of 1.8×10^5 psi at 1.7×10^{-3} second ($\log\tau = -2.8$) is the same as that measured in tension, compression, and relaxation in this same time scale.

Data have been presented to show that the modulus obtained from three totally different experiments are equivalent if time, or the duration of the experiment, is considered to be the independent variable. For example, the modulus at $\tau = 1.7 \times 10^{-3}$ second was 1.8×10^5 psi in all three experiments. However, the strain rate, at the time the moduli were measured, varied from zero (stress relaxation test) to 3 in./in.-min (outer fiber of the resonant beam) to a high value of 10^3 in./in.-min (high strain rate test). This implies that the modulus is not strain rate dependent.

Effect of Time and Temperature

In equations (1) and (2) it is assumed that the viscoeleastic solid is maintained at a uniform temperature. However, it is possible to incorporate the effect of temperature in the case of thermorheologically simple materials (ref. 4 and 6). In such a case a change of temperature is considered to be equivalent to a shifting of the logarithmic time scale. For the relaxation functions of equations (1) and (2)

$$G_i(\tau,T) = \gamma_i [\ln\tau + \psi(\tau)] \qquad (3)$$

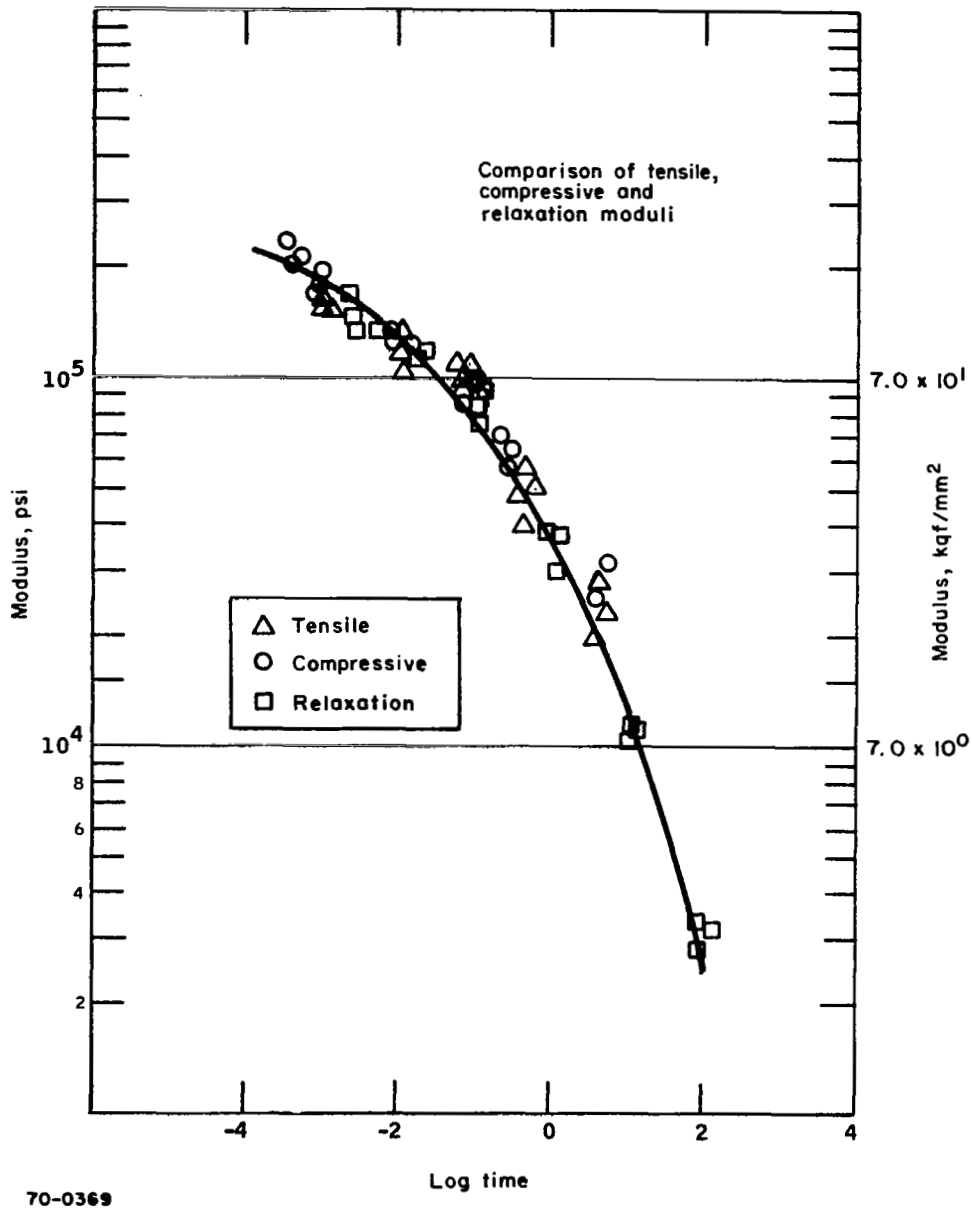

Figure 6 COMPARISON OF MODULI VERSUS TIME

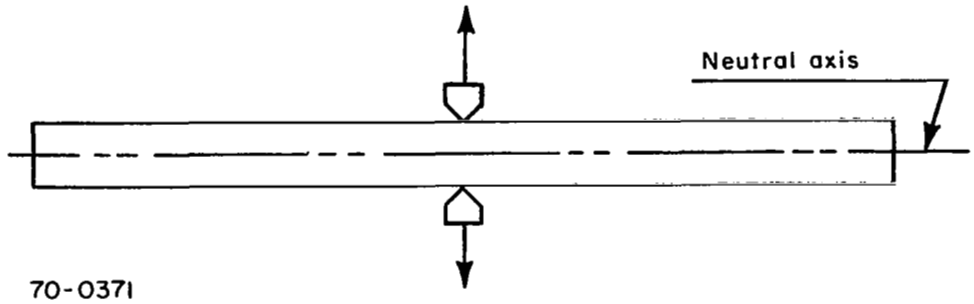

Figure 7 DOUBLE CANTILEVER BEAM

where the function $\psi(T)$ has the properties

$$\psi(T_o) = 0, \; d\psi/dT > 0 \tag{4}$$

for a reference temperature T_0. Then letting

$$\psi(T) = \ln \phi(T) \tag{5}$$

where $\phi(T)$ is a shift function with the properties

$$\phi(T_o) = 1, \; d\phi/dT > 0 \tag{6}$$

the relaxation function becomes

$$G_i(\tau,T) = \gamma_i[\ln \tau\phi] \tag{7}$$

for the constant temperature T. The shift function $\phi(T)$ is a positive, monotonic increasing function of T and represents an intrinsic property of the viscoelastic solid. It is worth emphasizing that a change of temperature is equivalent to a shifting of the logarithmic time scale (ref. 6).

Time-temperature equivalence can be illustrated by means of the data presented in Figure 8. Figure 8 is a log-log plot of modulus versus time (τ) as measured in tension, compression, and relaxation at various temperatures using a flexible epoxy. Here it is seen that the modulus at 38°C in the time scale from 10^{-4} to 10^{0} second changes with temperature in about the same manner as that measured at 24°C in the time scale of 10^{-2} to 10^{2} seconds. The modulus has been affected by a constant temperature change only by a corresponding change in the logarithmic time scale. The same argument can be given for all the data in Figure 8.

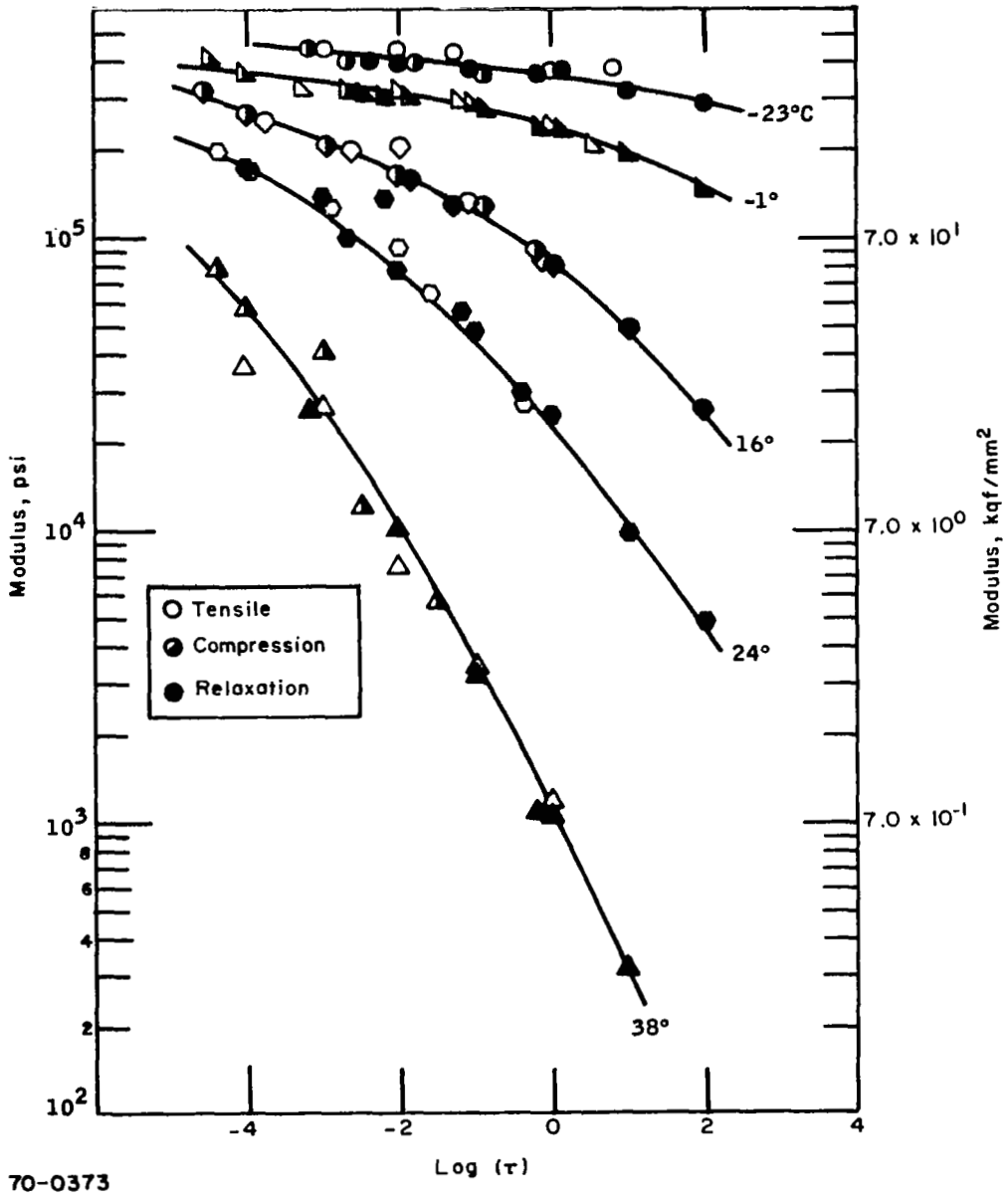

Figure 8 MODULUS VERSUS TIME AT VARIOUS TEMPERATURES

According to reference 6, the time and temperature dependence of the material can be combined mathematically to obtain a description of modulus in the form of equation (7). This combining can be done graphically also by shifting the curves of Figure 8 along the time scale until a single "master" curve is obtained as shown in Figure 9. (The details of the curve shifting and the generating of the master curve are given in Appendix B.) Figure 9 is a log-log plot of modulus versus a new parameter (τ /K) where τ is time and (1/K) is a temperature dependent parameter equivalent to the shift function ϕ(T) of equation (6). Figure 10 is a plot of log (1/K) versus the reciprocal of absolute temperature (degrees Kelvin). Here it is seen that the shift function (1/K) is a well behaved function of temperature and meets the requirements that

$$\phi(T_0) = 1 \quad (T_0 \text{ is a reference temperature, taken as room temperature in this case})$$

$$\frac{d\phi}{dT} > 0 \text{ for all } T .$$

Note that the shift function of Figure 10 exhibits two linear regions with a break at about 277^{0}K (4^{0}C). Previous work with polyethylene crystals (ref. 7) is associated with a second order phase change in the material.

The parameter (τ /K) in Figure 9 is both a time and a temperature term. For a given value of log (1/K) (i.e., for a constant temperature), the data in Figure 8 show the variation in modulus, over 16 orders of magnitude in time, at that constant temperature. Room temperature (24°C) has been arbitrarily chosen as the reference temperature (T_0), and hence the value of (1/K) is equal to 1.0, (τ /K) = τ and log (τ/K) = log(τ). At room temperature, then, the curve in Figure 9 represents the time dependency of the modulus from 10^{-12} to 10^{4} seconds. In order to determine the modulus for some particular time and temperature it is necessary to determine the appropriate value of (1/K) from Figure 10 for the desired temperature and then solve the equation

$$\text{Log}(\tau/K) = \text{Log } t + \text{Log}(1/K). \tag{8}$$

For example, the following procedure would be followed to determine the modulus at a frequency of 6 kHz and a temperature of 38°C:

1. 38°C = 311°K
2. 1/311 = 3.215 x 10^{-3}/°K
3. At 1/311 °K = 3.215 x 10^{-3}/°K, log (1/K) = 2.5
4. At a frequency of 6 kHz, the time τ is is one-fourth the period $(1/4 \times \frac{1}{6000})$ or τ = 4.2 x 10^{-5} second and Log (τ) = -4.4
5. Consequently Log (τ/K) = 4.4 + 2.5 = -1.9

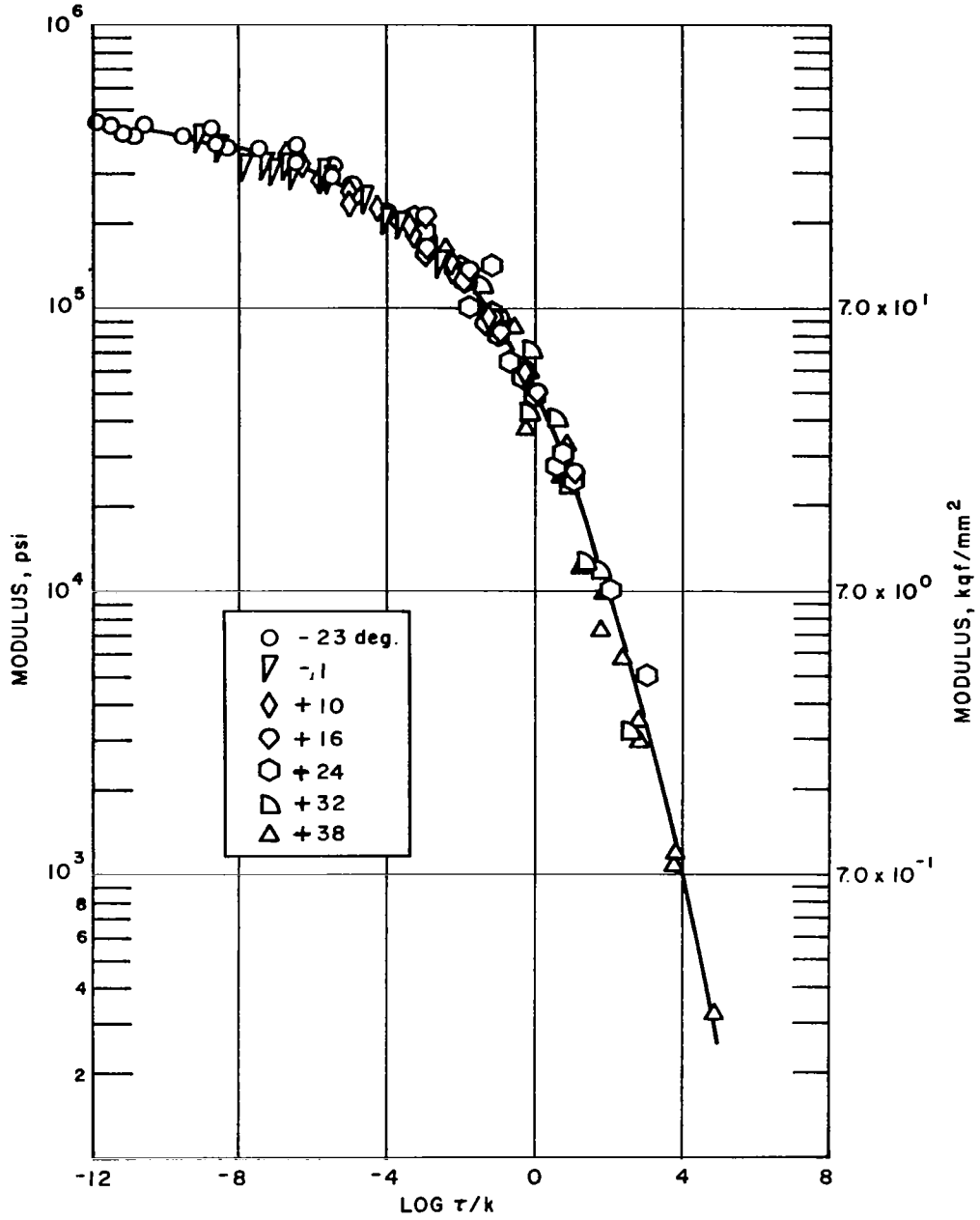

Figure 9 MASTER CURVE OF MODULUS

Referring to Figure 9, for a value of Log (τ /K) of -1.9, the modulus is 1.2 x 10^5 psi. This same approach will be used to compare the stress relaxation modulus and dynamic modulus in the following sections of this report.

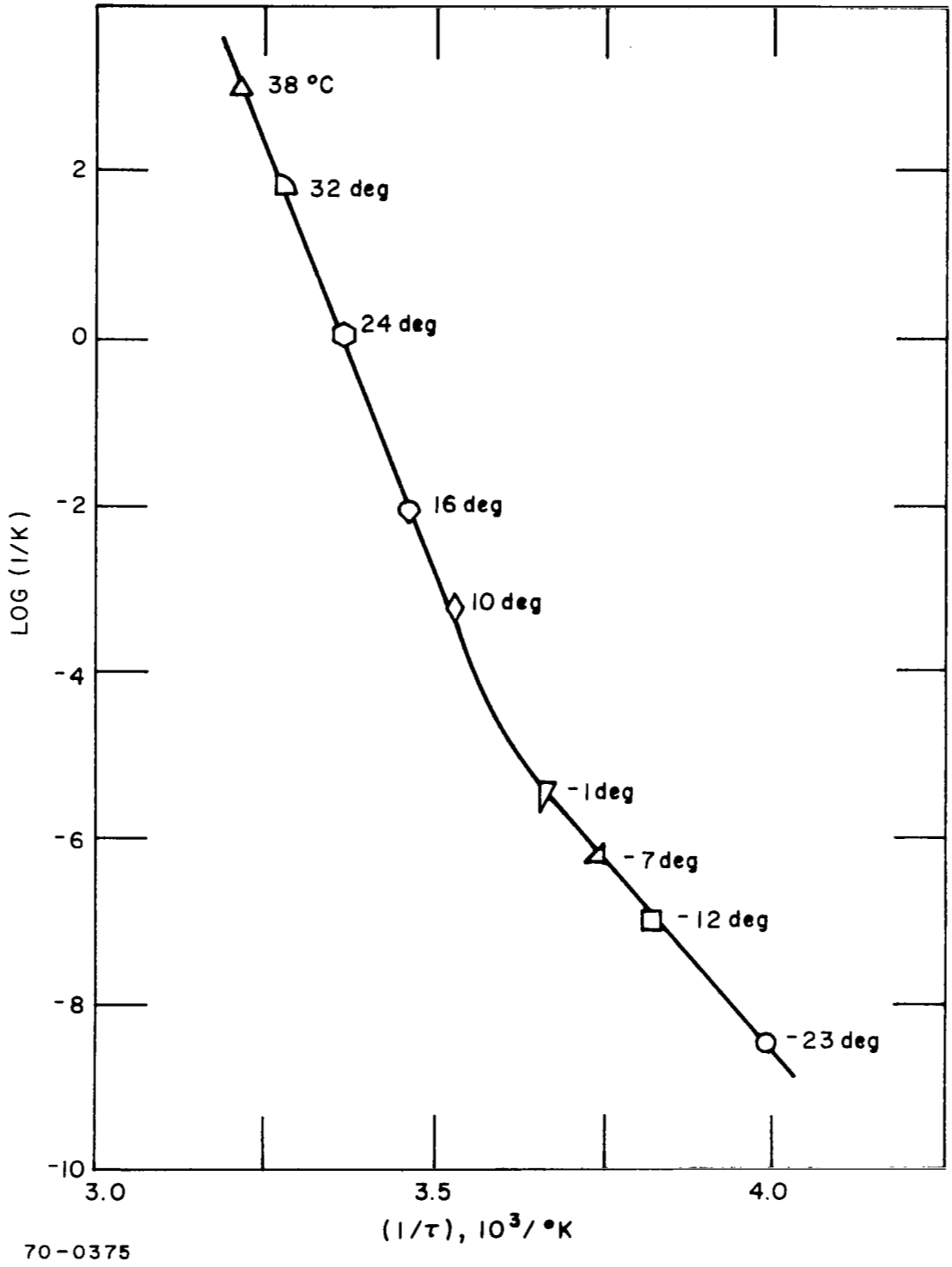

Figure 10 SHIFT FUNCTION

RESULTS AND DISCUSSION

The dynamic modulus and damping factor of 89 Pyrrone and polyimide molded specimens were measured at 5°K increments over the temperature range of 100° to 500°K. The stress relaxation modulus for 66 of these specimens was measured at 50°K increments over the range of 350° to 500°K, and at 20°K increments over the range of 500° to 700°K. The relaxation modulus of an additional 5 specimens was measured at 20°K increments over the range of 160° to 700°K. The thermal expansion of 27 of the 89 specimens was measured over the temperature range of 100° to 500°K.

Pyrrone Moldings

Pyrrone A.- The average dynamic modulus and the damping factor of 13 test specimens are listed in Table 1 and plotted as functions of temperature in Figure 11. Here it is seen that the modulus decreases almost linearly with temperature. There is a very broad peak in the damping curve covering the range from 100° to above 350°K with a maximum at 280°K. The small peak at 390°K is not consistent in that it appears in less than 50 percent of the samples.

The average stress relaxation modulus of 13 specimens is listed in Table 2. The values are reported at the 1.0, 10.0, and 100.0 second intervals. These data were superimposed using the superposition principal discussed earlier and the curve fitting technique described in Appendix B. The resulting master curve is shown in Figure 12. Here only the data points at 40°K intervals are denoted with symbols. The intermediate temperature points are not keyed. The shift function found for this material is shown as a function of reciprocal temperature in Figure 13. As mentioned earlier, the choice of a reference temperature is arbitrary. The reference temperature chosen for this material and all others to be presented is 500°K.

Unlike the shift function for the flexible epoxy (Figure 10), the shift function for the Pyrrone "A" polymer (Figure 13) exhibits very little linearity in the range of 160° to 500°K ($6.25 \times 10^{-3} \leq 1/T \leq 2.0 \times 10^{-3}$). This would be indicative of very gradual transitions or broad transition temperatures. Figure 14 is a straight-line approximation to the shift function. Here pseudo transitions are observed at 275°, 390°, 578°, and 600°K. The pseudo transition at 275°K agrees very well with the peak in the damping curve at 280°K. The second pseudo transition at 390°K is also in good agreement with either the minimum or small peak in the damping curve at 390°K.

Following the approach outlined earlier using the master curve of modulus versus log (τ/K) and the shift function, the modulus at a frequency of 6.0 kHz at various temperatures can be predicted. The first step is to solve the relationship:

$$\text{Log } (\tau/K) = -4.6 + \text{Log } (1/K)$$

TABLE 1

DYNAMIC MODULUS AND DAMPING FACTOR OF PYRRONE A

Temperature, ^{o}K	Dynamic Modulus, 10^6 psi	Damping Factor
100	1.23	.0118
110	1.23	.0127
120	1.22	.0137
130	1.22	.0140
140	1.20	.0156
150	1.20	.0145
160	1.19	.0178
170	1.18	.0199
180	1.17	.0226
190	1.16	.0267
200	1.14	.0289
210	1.13	.0290
220	1.13	.0320
230	1.11	.0353
240	1.09	.0384
250	1.08	.0394
260	1.07	.0412
270	1.06	.0420
280	1.05	.0429
290	1.03	.0397
300	1.02	.0365
310	1.01	.0322
320	1.00	.0289
330	.98	.0283
340	.97	.0261
350	.96	.0252
360	.94	.0238
370	.93	.0215
380	.92	.0244
390	.90	.0267
400	.89	.0239
410	.89	.0252
420	.88	.0272
430	.87	.0312
440	.86	.0356
450	.85	.0390
460	.84	.0431
470	.83	.0468
480	.82	.0501
490	.81	.0544
500	.79	.0625

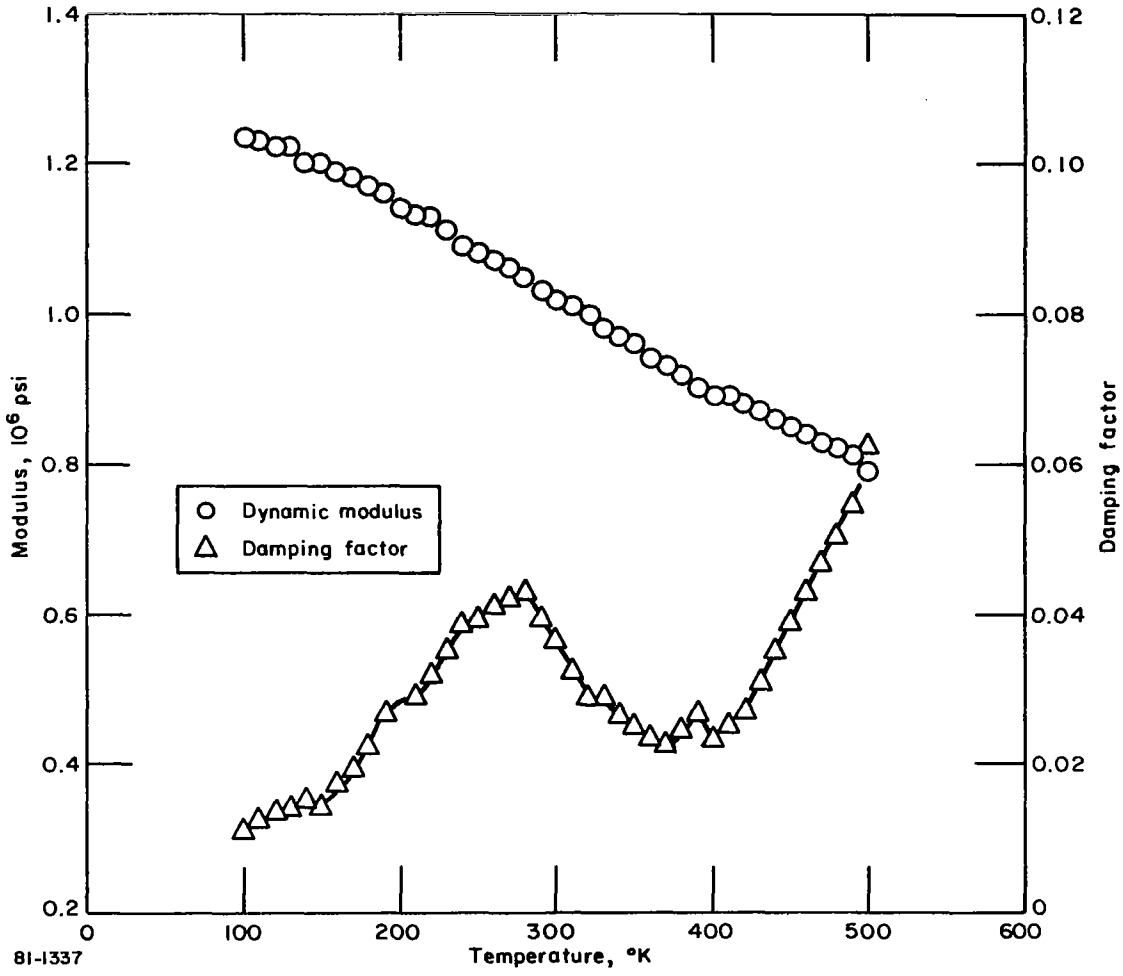

Figure 11 DYNAMIC MODULUS AND DAMPING FACTOR OF PYRRONE A

TABLE 2

RELAXATION MODULUS AND SHIFT FACTOR OF PYRRONE A

Temperature, ^{o}K	Relaxation Modulus At-			Log (1/K)
	1 Sec, 10^6 psi	10 Sec, 10^6 psi	100 Sec, 10^6 psi	
160	1.11	1.09	1.04	-16.9
180	1.07	1.06	1.02	-15.9
200	1.05	1.04	1.00	-15.0
220	1.04	1.03	1.00	-14.1
240	1.01	1.01	.97	-13.3
260	1.00	.98	.96	-12.1
280	.97	.95	.92	-10.6
300	.95	.93	.90	-9.1
320	.90	.88	.86	-7.5
340	.88	.84	.80	-5.9
360	.81	.76	.70	-4.1
380	.77	.71	.65	-3.2
400	.70	.64	.58	-2.2
450	.60	.54	.47	-.9
500	.52	.46	.38	0
520	.50	.45	.37	.3
540	.48	.43	.34	.6
560	.45	.40	.31	1.0
580	.39	.33	.23	1.9
600	.32	.27	.18	2.6
620	.29	.23	.16	3.1
640	.26	.21	.15	3.4
660	.26	.22	.16	3.6
680	.25	.21	.15	3.9
700	.21	.17	.11	4.6

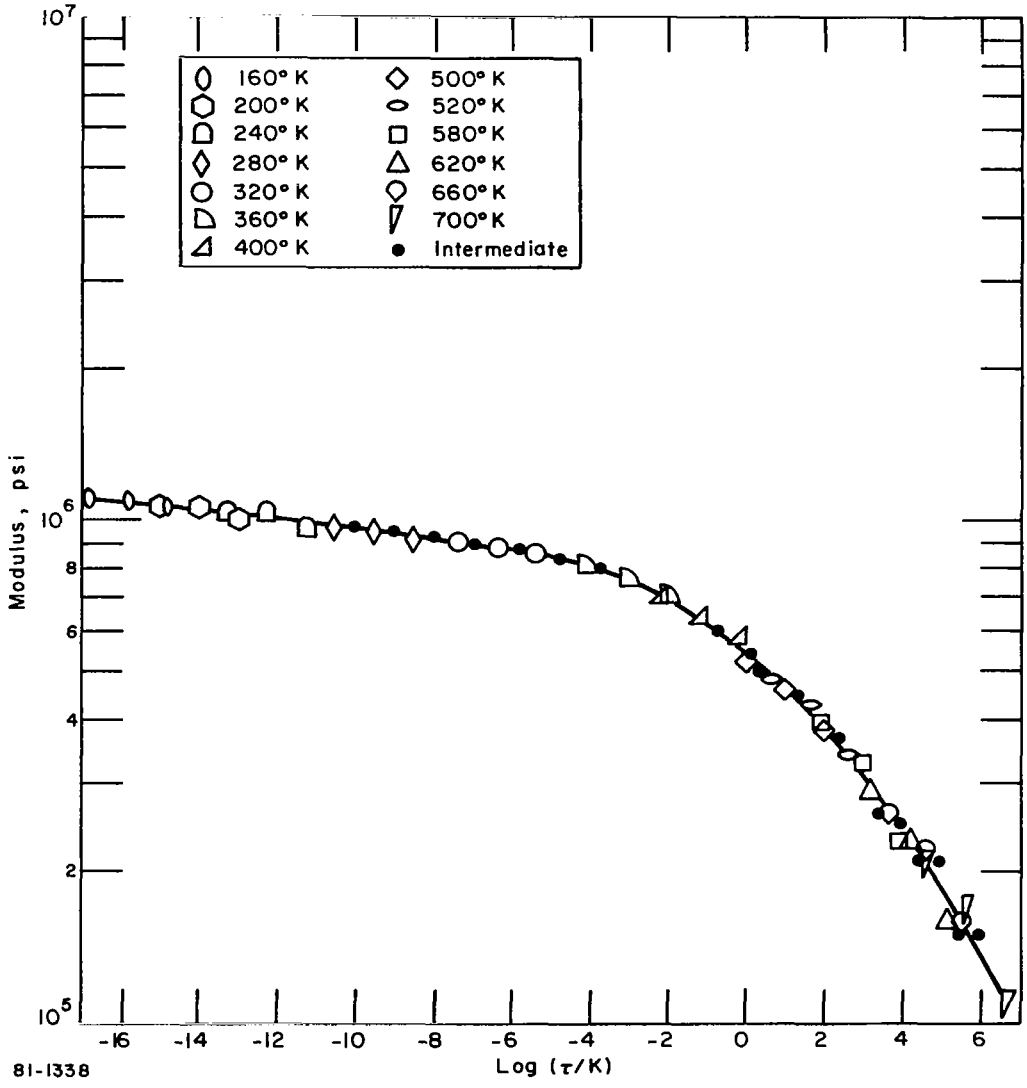

Figure 12 MASTER CURVE OF MODULUS OF PYRRONE A

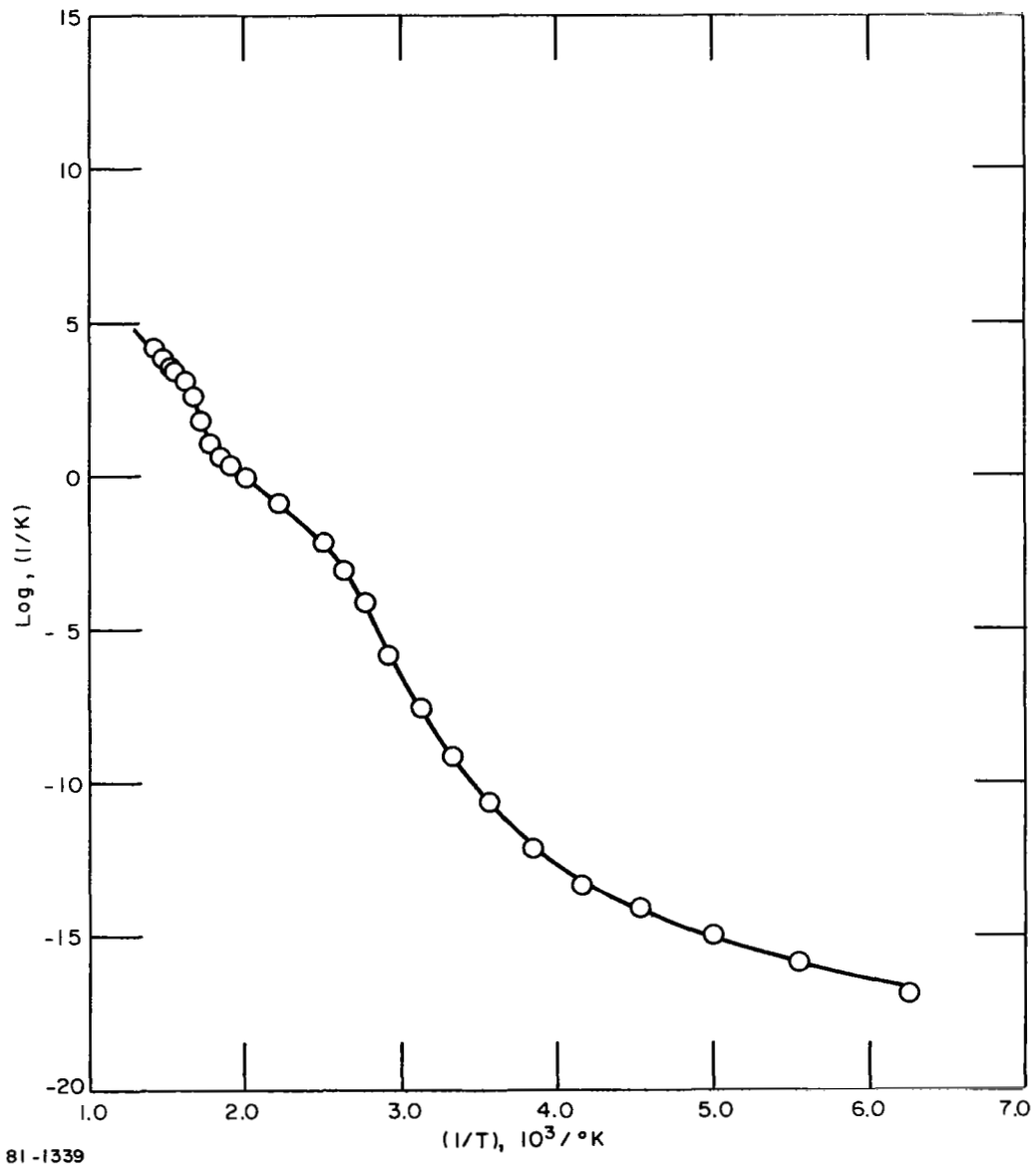

Figure 13 SHIFT FUNCTION OF PYRRONE A

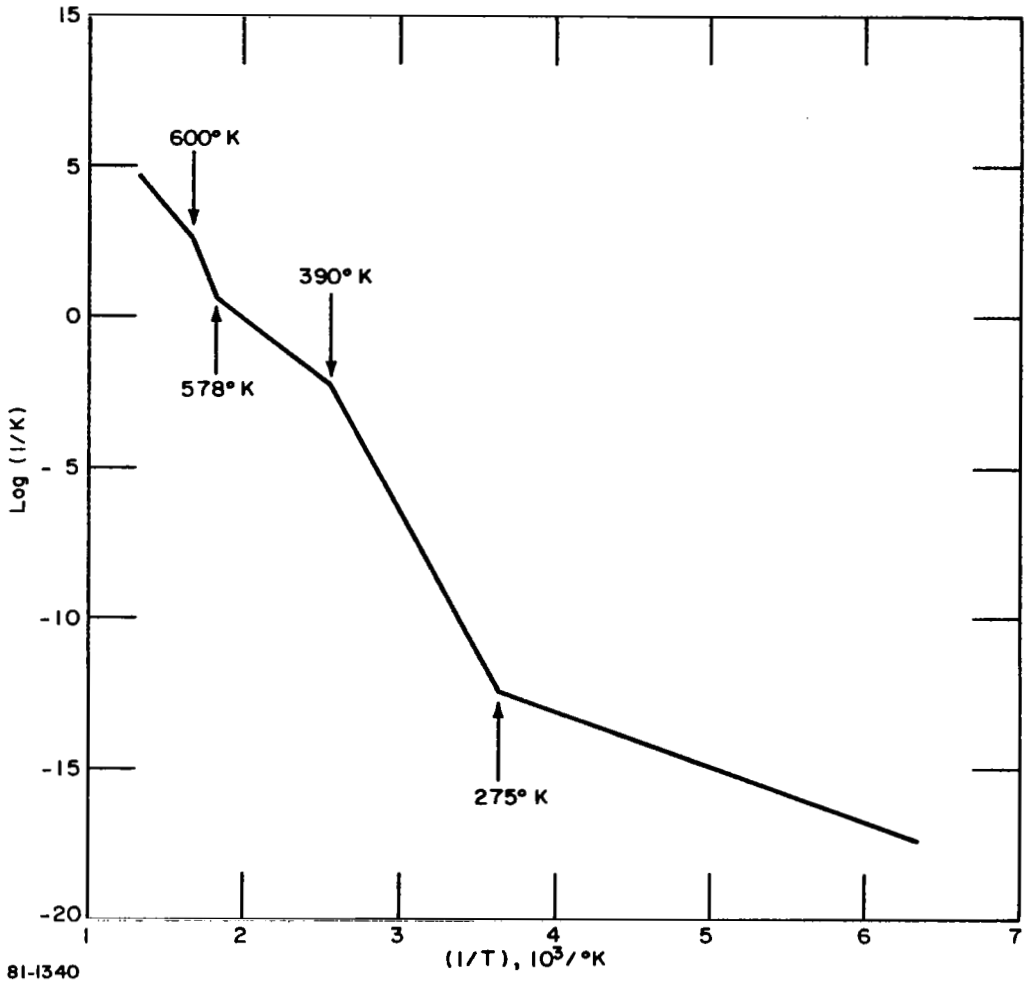

Figure 14 STRAIGHT LINE APPROXIMATION OF SHIFT FUNCTION OF PYRRONE A

The minimum value Log (1/K) can have and still be in range of the master curve of Figure 12 is about -12. At 260°K ($1/T = 3.85 \times 10^{-3}$), Log (1/K) = -12.1. At Log (1/K) = -12.1, Log (τ/K) = -16.7. At a value of Log (τ/K) = -16.7 the modulus is 1.09×10^6 psi. This is within 2 percent of the measured value of 1.07×10^6 psi at 260°K.

Following this in a step-by-step fashion, predictions of the dynamic moduli at 20°K increments from 260° to 700°K were made. Figure 15 is a comparison between the measured and predicted moduli over the temperature range from 100° to 700°K. The measured and predicted values fall within 3 percent of each other within the common temperature range (260° to 500°K).

The average thermal expansion of 2 specimens is listed in Table 3 and plotted as a function of temperature in Figure 16. Using straight-line approximations, transitions are apparent at 280° and 390°K.

Pyrrone A with 15 weight percent graphite powder.- The average dynamic modulus and damping of eight test specimens are listed in Table 4 and plotted as functions of temperature in Figure 17. Here it is seen that the graphite powder increased to modulus by about 26 percent over the entire temperature range as compared with the Pyrrone A without graphite. The damping factors in the range from 300° to 500°K are slightly higher, but there are no significant differences in the general shape of the damping curve. The average relaxation moduli of eight test specimens are listed in Table 5. The master curve constructed from these data is shown in Figure 18. No significant difference in the shift function was observed due to the graphite powder. The similarity between the damping curves and the shift function curves implies that the addition of the graphite powder does not influence or alter the structure of the Pyrrone A moldings.

Pyrrone L.- The average dynamic modulus and the damping factor of 26 test specimens are listed in Table 6 and shown as functions of temperature in Figure 19. In Figure 19 it is seen that not only does the modulus start out at a lower level than the Pyrrone A (1.0×16^6 versus 1.2×10^6), but also the rate of change in modulus with temperature in the range from 200° to 300°K is greater. The damping peak in the range of 200° to 300°K is about a factor of two higher than observed on the Pyrrone A. These features would indicate that the molecular changes associated with these second order phases, although similar in the two materials, is more extensive in the Pyrrone L.

The average stress relaxation modulus of 24 test specimens over the temperature range of 350° to 700°K are listed in Table 7. The master curve constructed from these data is shown in Figure 20. There are two characteristics of this shift function in Figure 21 which differ from that established for the Pyrrone A (Figure 13). In the temperature range below 500°K ($1/T > 2.0 \times 10^{-3}$), the slope of the Pyrrone L shift function is lower. There appears to be a transition at about 570°K which is in good agreement with that observed for the Pyrrone A; however, there is no evidence of a transition at 600°K. Figure 22 is a comparison between the measured and predicted dynamic moduli. In the range from 350° to 450° the predicted values are within 2 percent of the measured values. In the range from 450° to 500°K the agreement is not as good but is still within 10 percent.

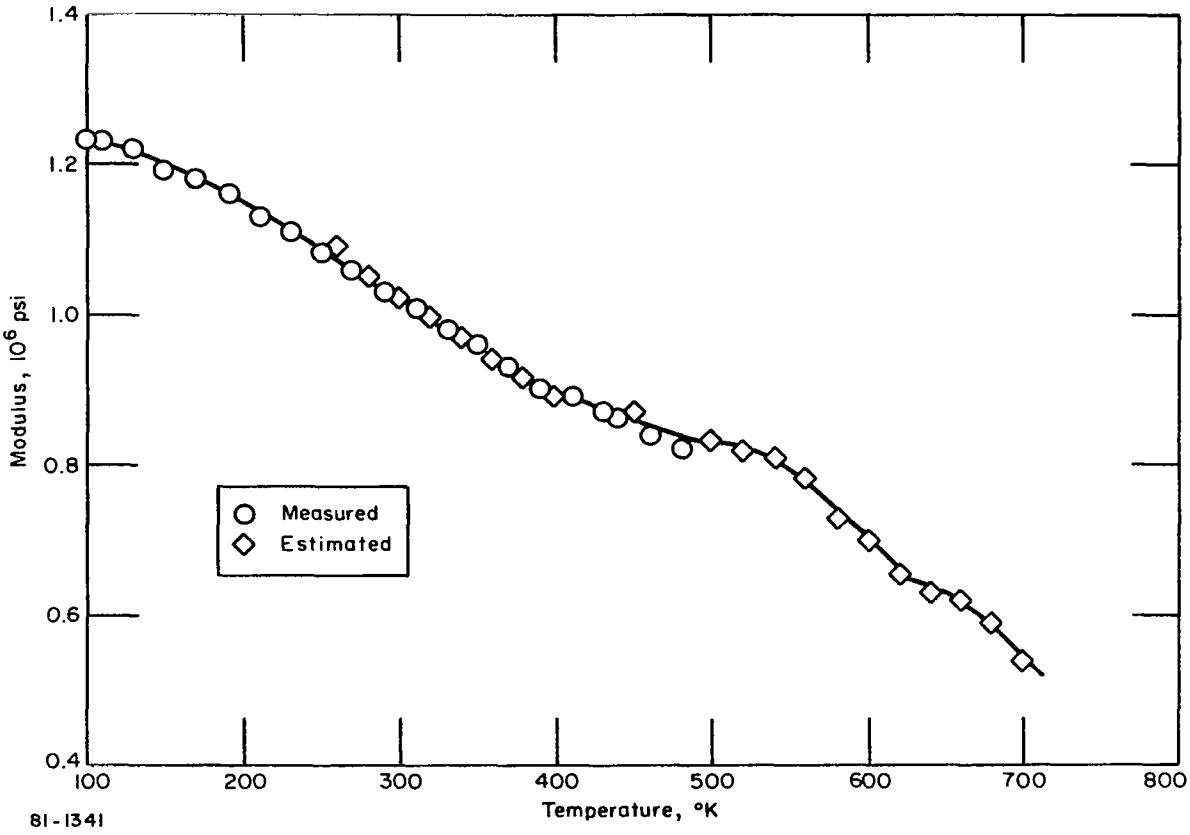

Figure 15 COMPARISON OF ESTIMATED AND MEASURED DYNAMIC MODULI OF PYRRONE A

TABLE 3

THERMAL STRAIN OF PYRRONE A

Temperature, ^{o}K	Strain, %
100	-.472
111	-.452
122	-.438
133	-.417
144	-.388
155	-.366
166	-.341
177	-.315
189	-.290
200	-.267
211	-.239
222	-.200
233	-.188
244	-.156
255	-.129
266	-.100
277	-.065
289	-.028
300	0
311	.036
322	.072
333	.106
344	.152
355	.193
366	.237
377	.267
389	.300
400	.321
411	.333
422	.348
433	.352
444	.357
455	.356
466	.352
477	.350
489	.350
500	.354

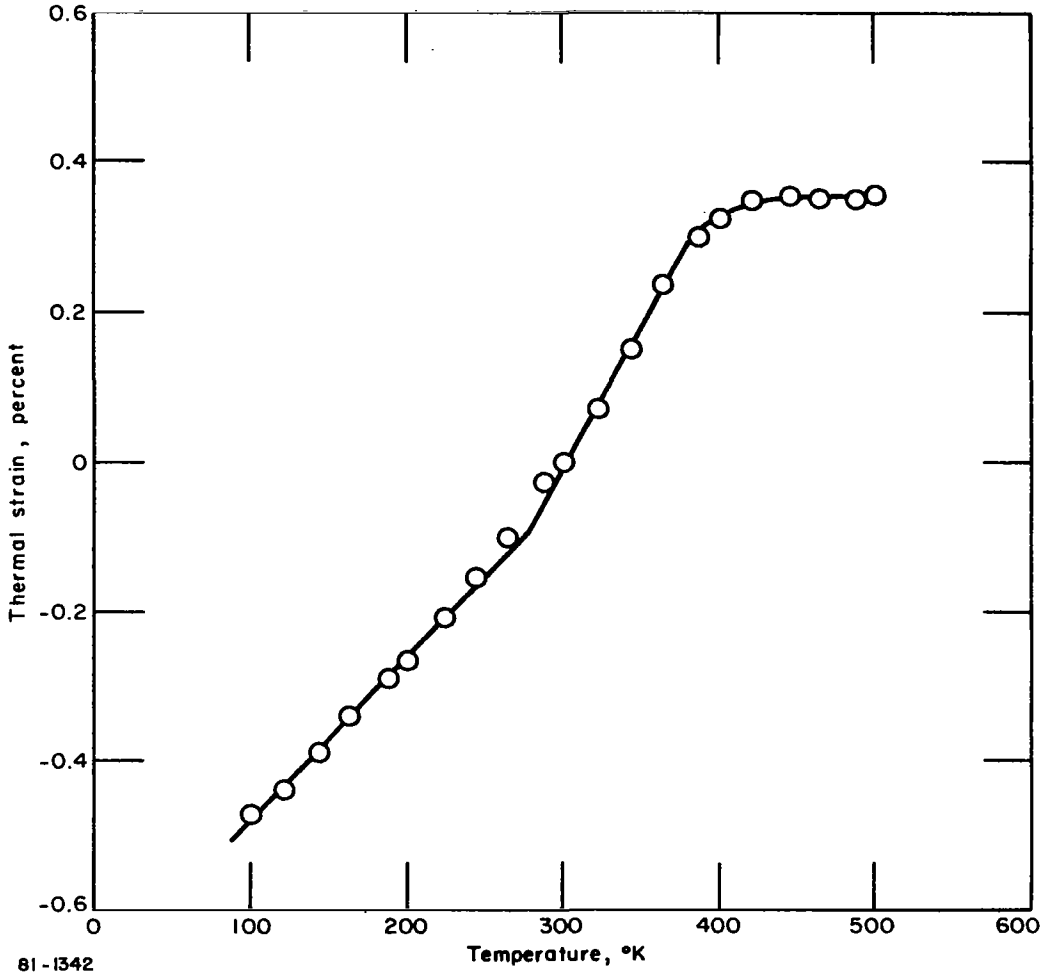

Figure 16 THERMAL STRAIN VERSUS TEMPERATURE OF PYRRONE A

TABLE 4

DYNAMIC MODULUS AND DAMPING FACTOR OF PYRRONE A WITH 15 WEIGHT PERCENT GRAPHITE POWDER

Temperature, ^{o}K	Dynamic Modulus, 10^{6} psi	Damping Factor
100	1.56	.0120
110	1.56	.0122
120	1.55	.0130
130	1.54	.0140
140	1.53	.0135
150	1.52	.0155
160	1.51	.0164
170	1.50	.0169
180	1.48	.0185
190	1.47	.0221
200	1.45	.0248
210	1.43	.0293
220	1.42	.0331
230	1.40	.0346
240	1.38	.0374
250	1.36	.0388
260	1.34	.0423
270	1.33	.0447
280	1.31	.0410
290	1.29	.0402
300	1.27	.0378
310	1.25	.0353
320	1.23	.0320
330	1.21	.0307
340	1.20	.0302
350	1.18	.0286
360	1.17	.0283
370	1.15	.0302
380	1.14	.0313
390	1.13	.0318
400	1.12	.0332
410	1.10	.0340
420	1.09	.0355
430	1.08	.0410
440	1.07	.0410
450	1.06	.0441
460	1.05	.0468
470	1.03	.0508
480	1.01	.0532
490	.99	.0592
500	.97	.0668

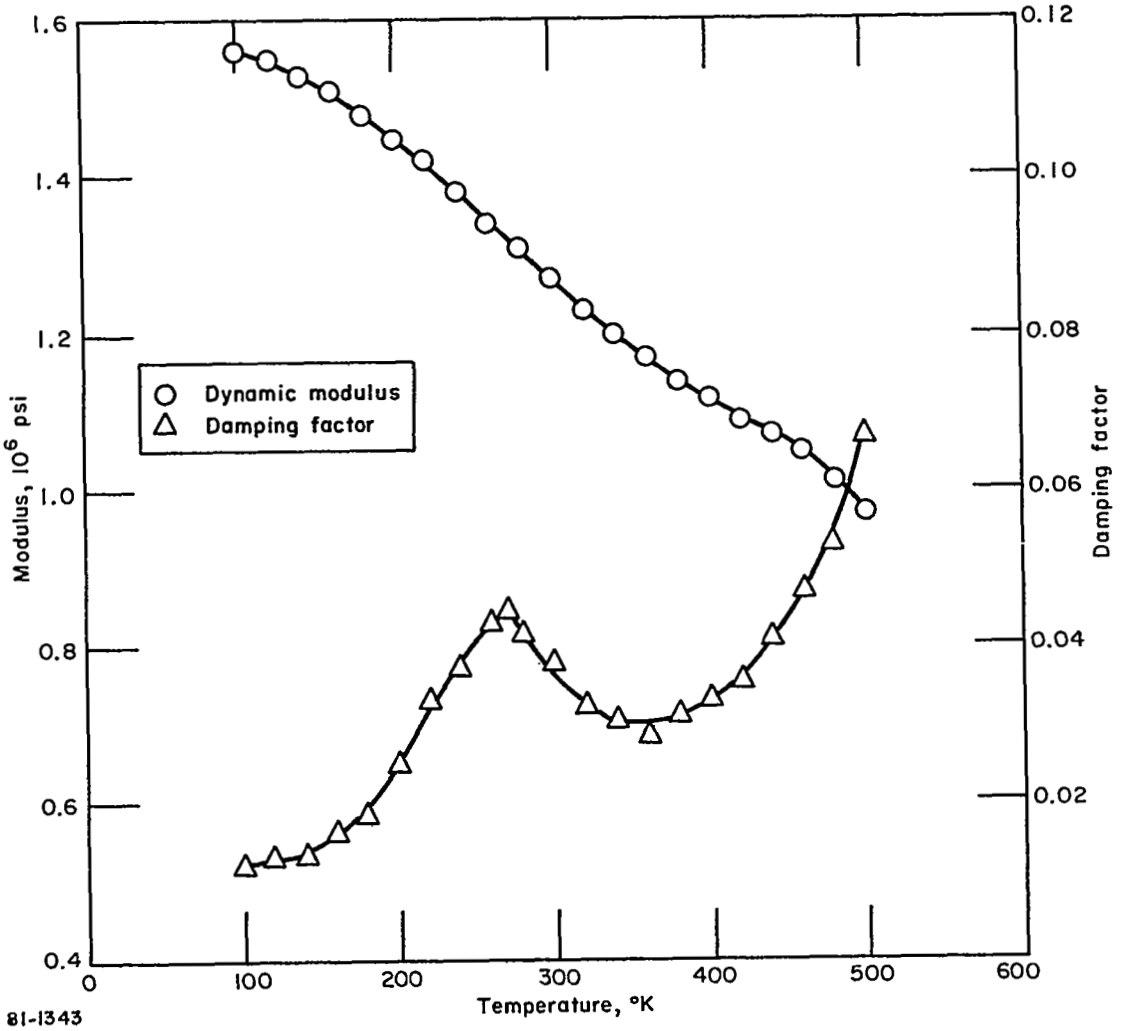

Figure 17 DYNAMIC MODULUS AND DAMPING FACTOR OF PYRRONE A WITH 15 WEIGHT PERCENT GRAPHITE POWDER

TABLE 5

RELAXATION MODULUS OF PYRRONE A
WITH 15 WEIGHT PERCENT GRAPHITE POWDER

Temperature, ^{o}K	Relaxation Modulus At-		
	1 Sec, 10^6 psi	10 Sec, 10^6 psi	100 Sec, 10^6 psi
160	1.26	1.23	1.19
180	1.22	1.20	1.15
200	1.19	1.16	1.12
220	1.14	1.13	1.09
240	1.13	1.12	1.06
260	1.11	1.08	1.04
280	1.06	1.05	1.01
300	1.02	1.01	1.00
320	.99	.98	.96
340	.92	.90	.87
360	.86	.82	.76
380	.82	.78	.72
400	.77	.72	.66
450	.69	.63	.56
500	.64	.58	.49
520	.64	.58	.50
540	.64	.57	.47
560	.60	.53	.42
580	.53	.45	.34
600	.49	.42	.32
620	.45	.39	.30
640	.42	.36	.28
660	.39	.33	.25
680	.36	.30	.22
700	.32	.26	.19

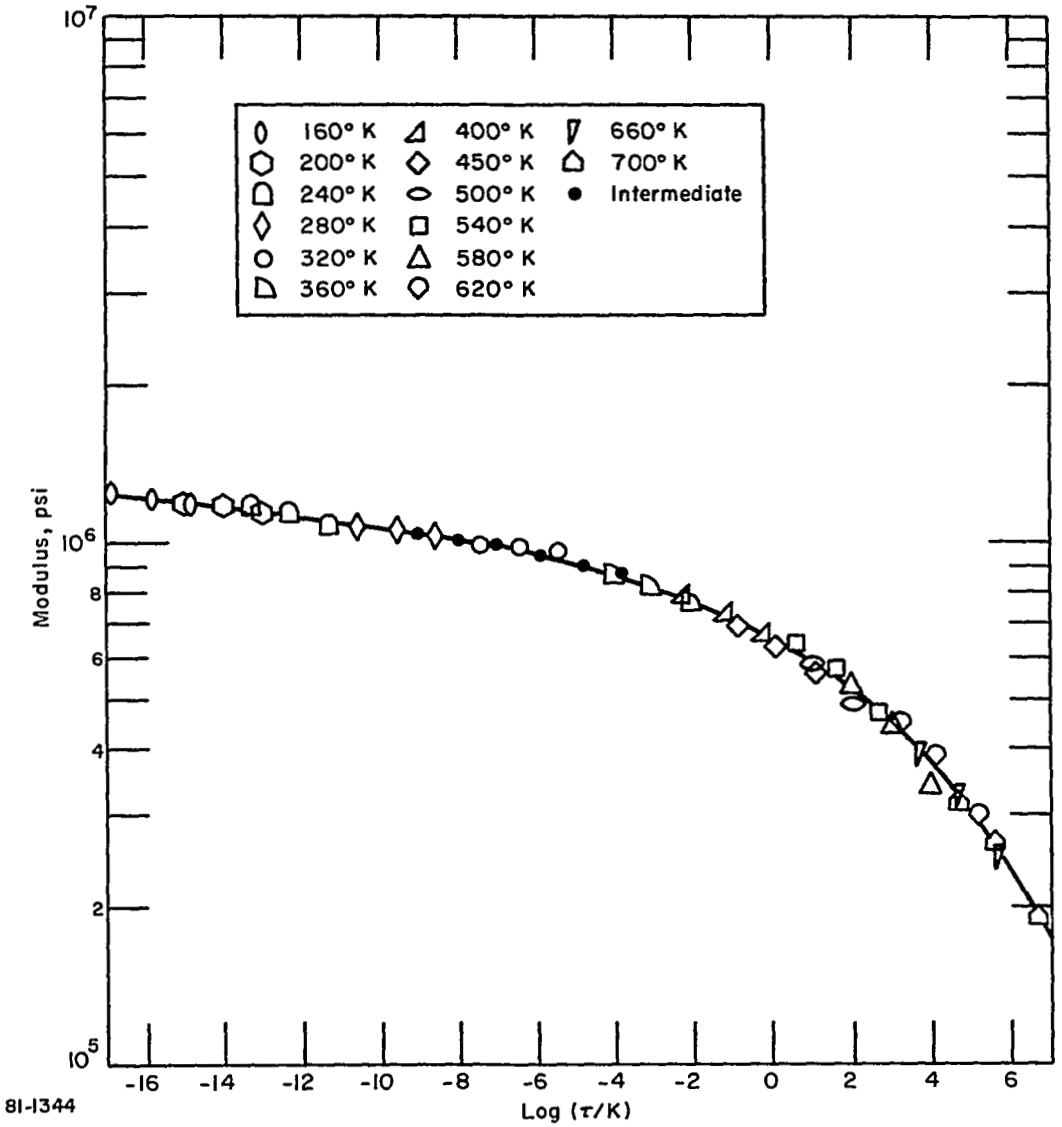

Figure 18 MASTER CURVE OF MODULUS OF PYRRONE A WITH 15 WEIGHT PERCENT GRAPHITE POWDER

TABLE 6

DYNAMIC MODULUS AND DAMPING FACTOR OF PYRRONE L

Temperature, ^{o}K	Dynamic Modulus, 10^6 psi	Damping Factor
100	.999	.0130
110	.993	.0138
120	.985	.0161
130	.975	.0177
140	.962	.0199
150	.945	.0242
160	.937	.0290
170	.921	.0367
180	.903	.0419
190	.893	.0452
200	.867	.0562
210	.848	.0606
220	.829	.0703
230	.806	.0796
240	.784	.0779
250	.767	.0769
260	.749	.0783
270	.736	.0693
280	.725	.0558
290	.713	.0463
300	.702	.0384
310	.686	.0296
320	.674	.0284
330	.660	.0282
340	.650	.0278
350	.638	.0258
360	.631	.0255
370	.623	.0261
380	.615	.0253
390	.615	.0266
400	.610	.0271
410	.606	.0254
420	.603	.0255
430	.597	.0273
440	.593	.0282
450	.587	.0306
460	.579	.0331
470	.571	.0339
480	.562	.0339
490	.550	.0365
500	.535	.0418

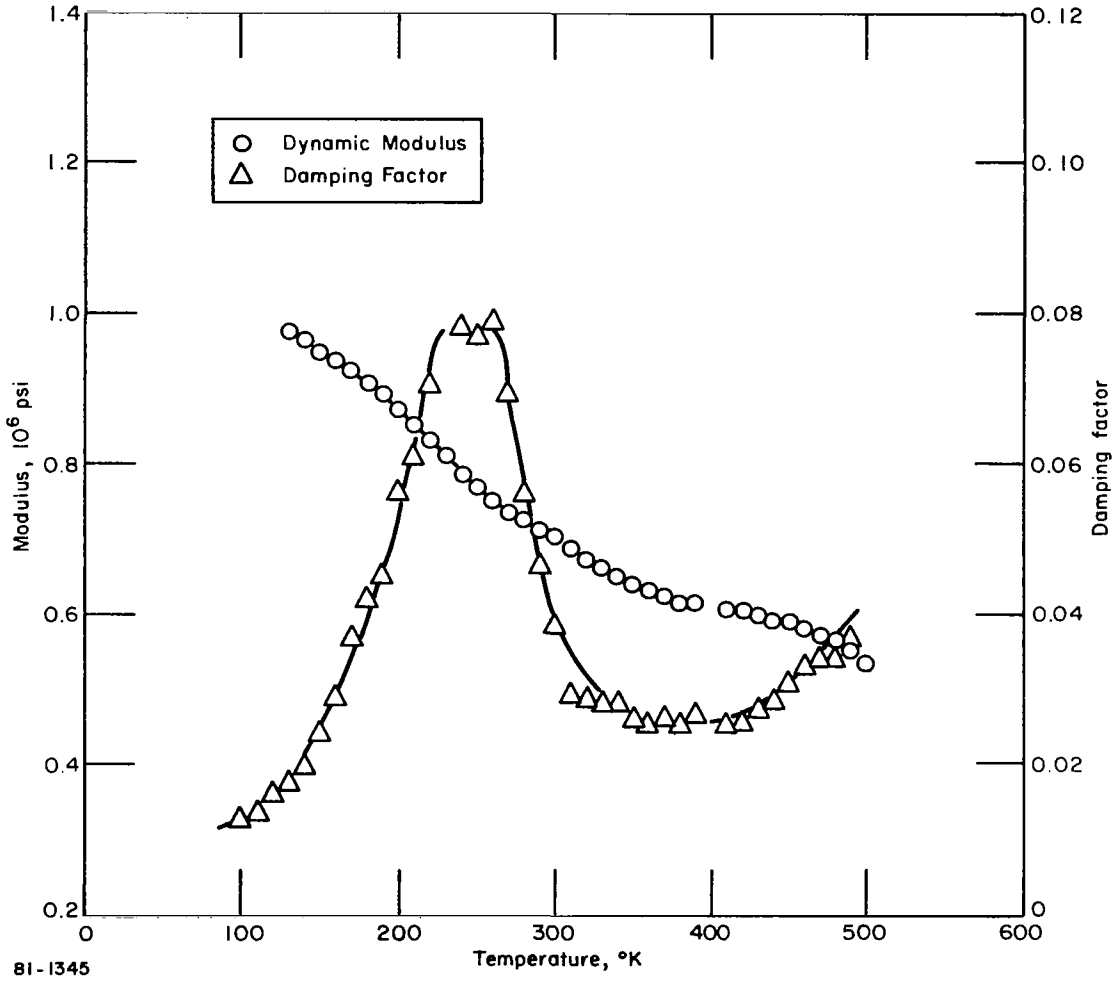

Figure 19 DYNAMIC MODULUS AND DAMPING FACTOR OF PYRRONE L

TABLE 7

RELAXATION MODULUS AND SHIFT FACTOR OF PYRRONE L

Temperature, ^{o}K	Relaxation Modulus At-			Log (1/K)
	1 Sec, 10^6 psi	10 Sec, 10^6 psi	100 Sec, 10^6 psi	
350	.519	.487	.433	-1.95
400	.492	.456	.400	-.66
450	.480	.443	.392	-.21
500	.465	.427	.380	0
520	.444	.406	.363	.35
540	.425	.388	.342	.80
560	.409	.370	.328	1.00
580	.382	.344	.295	1.84
600	.362	.327	.274	2.36
620	.344	.308	.255	2.79
640	.324	.292	.235	2.41
660	.303	.272	.215	3.80
680	.286	.257	.197	4.50
700	.267	.242	.184	5.10

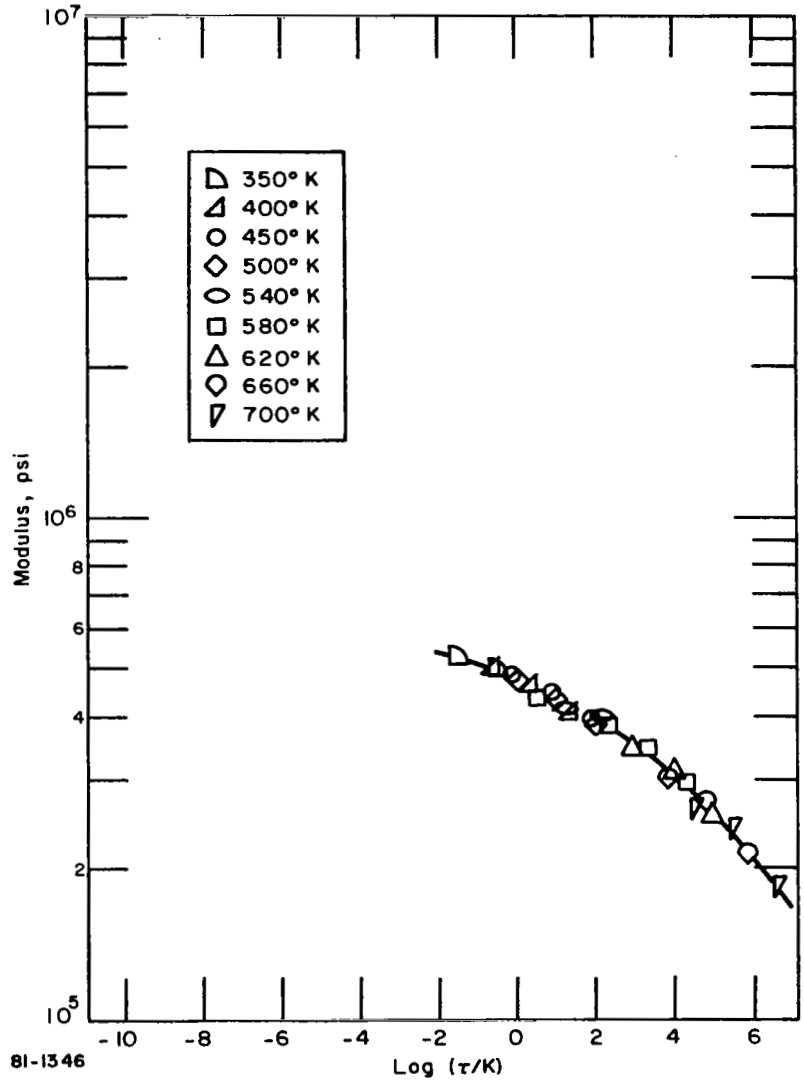

Figure 20 MASTER CURVE OF MODULUS OF PYRRONE L

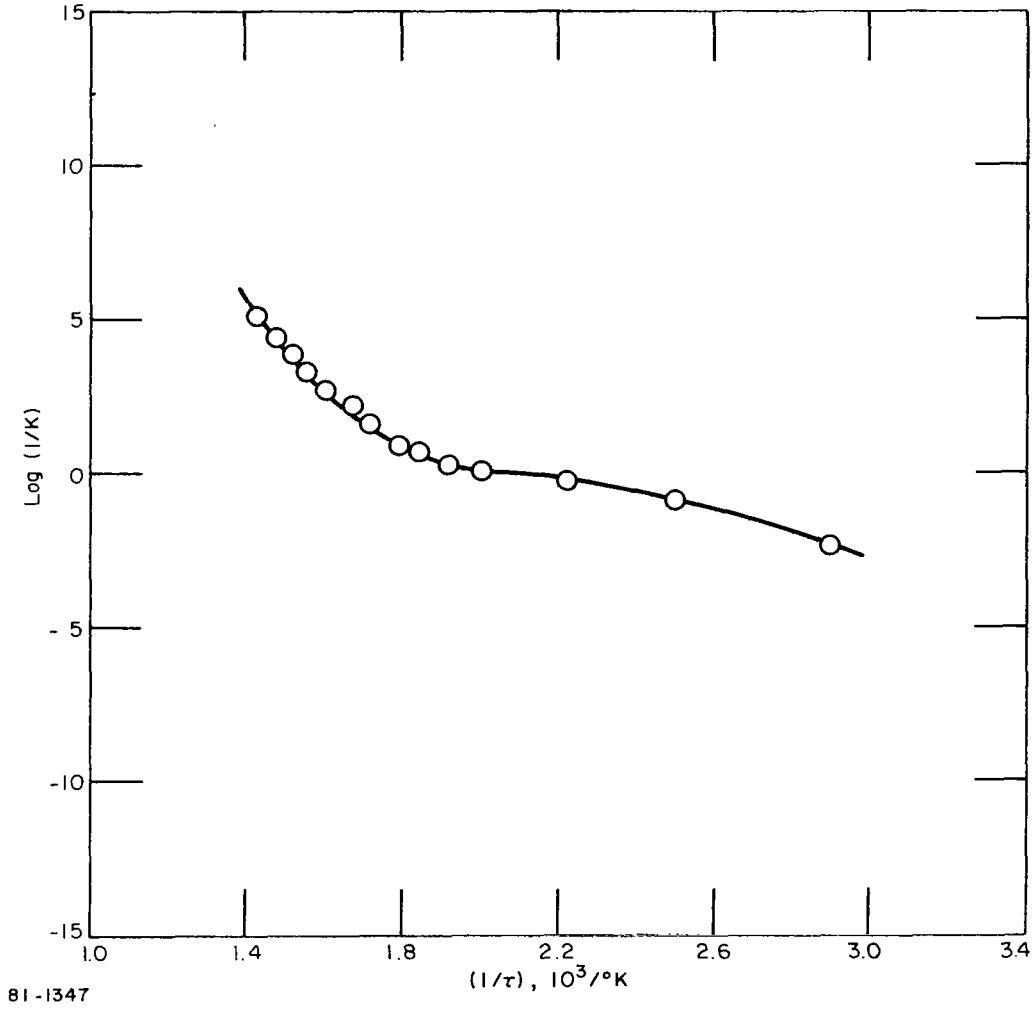

Figure 21 SHIFT FUNCTION OF PYRRONE L

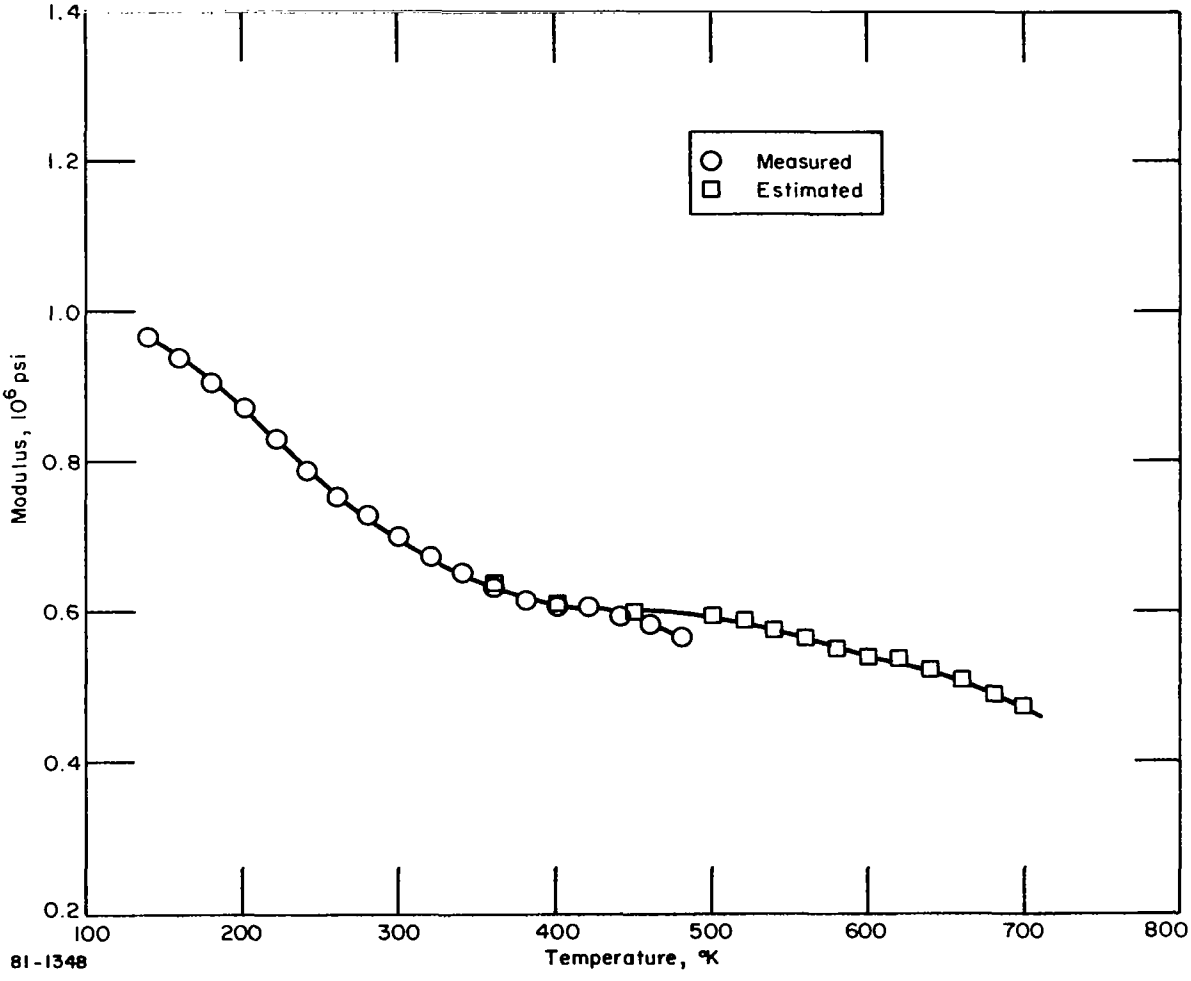

Figure 22 COMPARISON OF ESTIMATED AND MEASURED DYNAMIC MODULI OF PYRRONE L

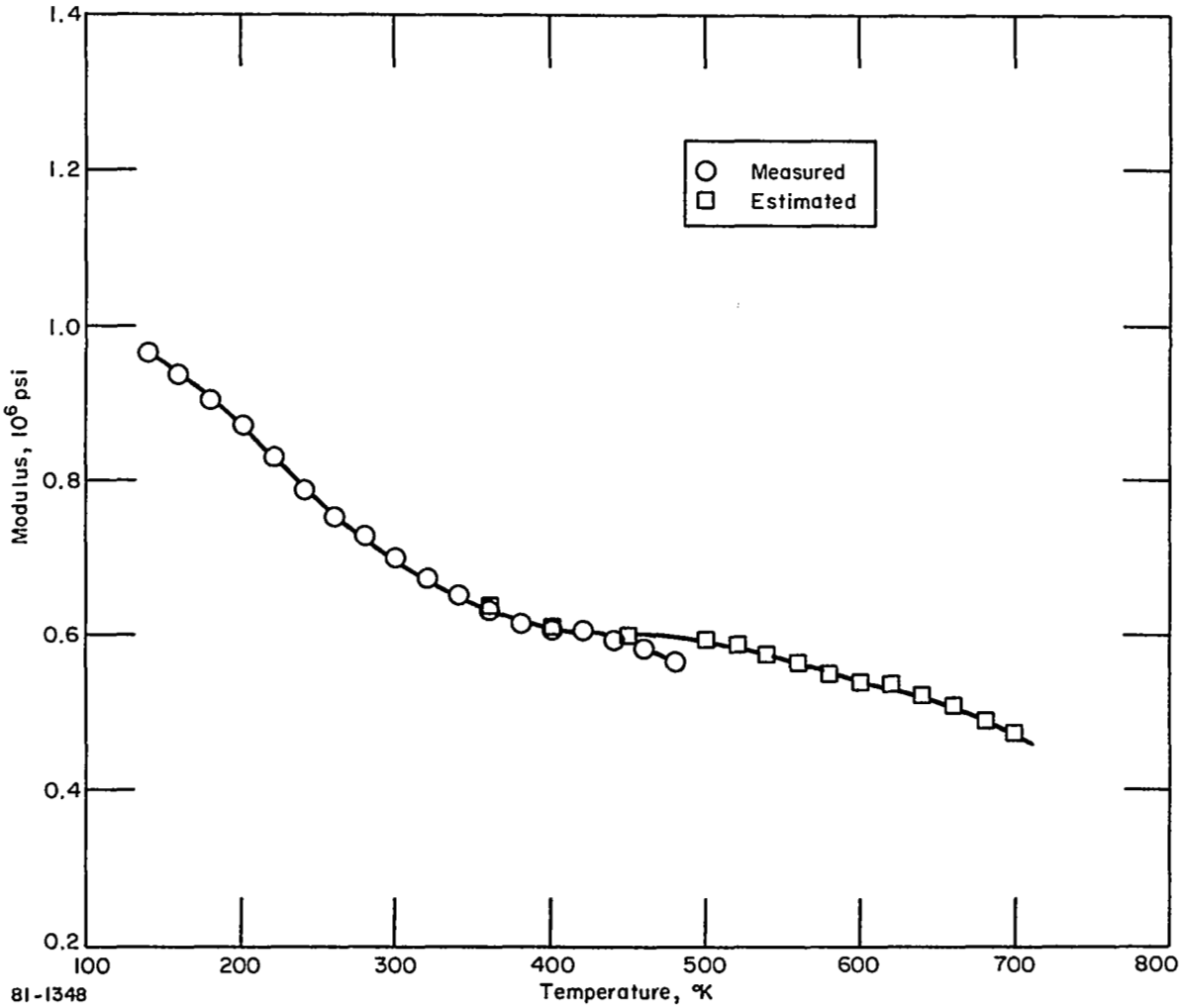

Figure 22 COMPARISON OF ESTIMATED AND MEASURED DYNAMIC MODULI OF PYRRONE L

The average expansion of 10 test specimens is listed in Table 8 and plotted in Figure 23. The thermal expansion characteristics of the Pyrrone L also differ from those observed for the Pyrrone A. There is a definite shrinkage in the range between 350° and 450°K which may be an indication of a loss of water which has a boiling point of 373°K. A small break in the curve in the range from 340° to 360°K is observed which is consistent with peak in the damping curve.

Polyimide Moldings

Polyimide B.- The average dynamic modulus and the damping factors of the 18 test specimens are listed in Table 9 and are plotted as functions of temperature in Figure 24. In Figure 24, it is seen the modulus varies almost linearly with temperature and the damping peak in the range between 200° and 300°K is less pronounced than observed in the Pyrrones, and is at a lower temperature (250°K versus 280°K).

The average stress relaxation modulus of 12 test specimens is listed in Table 10. Tests were performed at temperatures above 600°K; however, these data are not reported. Significant changes in the slope of the modulus-time curves were observed at temperatures above 600°F and the curves were no longer superimposable. These changes were probably due to chemical changes or degradation of the polymer at these temperatures. Some of the specimens also exhibited extensive cracks. With chemical changes and/or crack formation the assumptions inherent in the time-temperature superposition model used are violated and it is unlikely that the relaxation curves would be superimposable. Figure 25 shows the master curve which was constructed using the relaxation data to 600°K, and Figure 26 is a plot of the shift function. The only transition observed in the shift function is at 520°K. For this reason it is likely that there would be little change in the slope of the damping curve in the region between 350° and 500°K. Considering only the 350°, 400°, 450°, and 500°K damping factors it is seen they vary almost linearly with temperature.

Figure 27 shows the comparison between the measured and predicted values of dynamic moduli. The agreement between the two are not especially good. The variation in moduli with temperature in the range between 400° and 500°K are in good agreement, but the values of the predicted modulus are 14 percent lower than the measured modulus.

There are two possible explanations. As mentioned earlier, some of the specimens run in stress relaxation to temperatures in excess of 600°K cracked and split. Cracking in these specimens has been observed at temperatures as low as 560°K. No attempt was made to establish the temperature at which incipient cracks form. All the samples tested in stress relaxation had been to 500°K previously in the dynamic modulus and damping experiments. If incipient cracks had formed or were aggravated by the thermal cycling they would, in effect, reduce the modulus. The 14 percent difference could also be the result of experimental error. This material was first to be evaluated in stress relaxation under this study. During the study improvements were made

TABLE 8

THERMAL STRAIN OF PYRRONE L

Temperature, ^{o}K	Thermal Strain, %
100	-0.457
122	-0.415
144	-0.365
166	-0.317
189	-0.266
200	-0.243
222	-0.190
244	-0.134
266	-0.079
289	-0.024
300	0
322	0.050
344	0.092
366	0.117
389	0.105
400	0.089
422	0.034
444	0.039
466	0.044
489	0.067
500	0.089

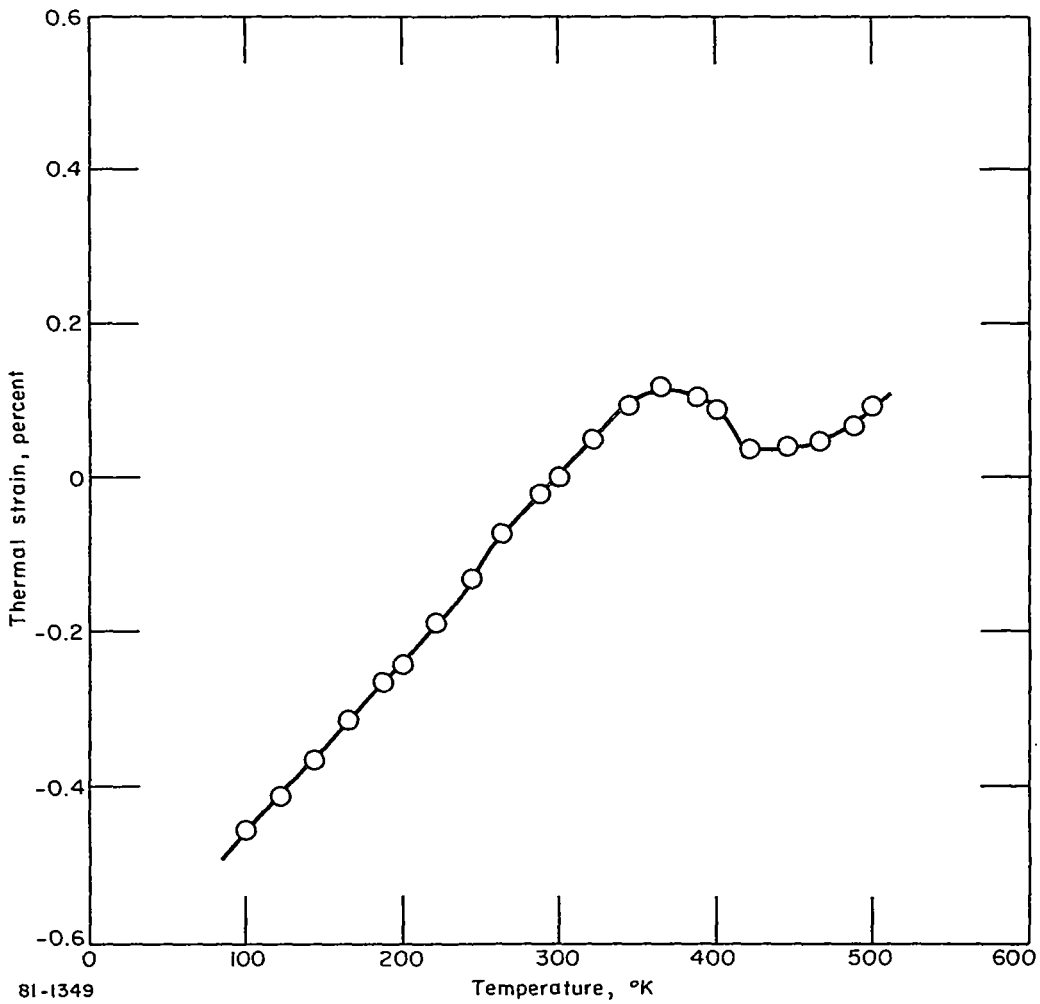

Figure 23 THERMAL STRAIN VERSUS TEMPERATURE OF PYRRONE L

TABLE 9

DYNAMIC MODULUS AND DAMPING FACTOR OF POLYIMIDE B

Temperature, ^{o}K	Dynamic Modulus, 10^6 psi	Damping Factor
100	1.013	.0089
110	1.007	.0091
120	1.000	.0096
130	.993	.0106
140	.984	.0116
150	.977	.0128
160	.968	.0146
170	.959	.0168
180	.948	.0196
190	.937	.0231
200	.926	.0254
210	.914	.0275
220	.903	.0329
230	.892	.0365
240	.880	.0374
250	.868	.0375
260	.860	.0359
270	.849	.0347
280	.840	.0330
290	.830	.0295
300	.822	.0279
310	.811	.0262
320	.802	.0244
330	.795	.0241
340	.786	.0259
350	.778	.0260
360	.770	.0286
370	.761	.0294
380	.751	.0314
390	.742	.0347
400	.734	.0354
410	.724	.0379
420	.714	.0412
430	.704	.0435
440	.695	.0467
450	.685	.0520
460	.676	.0573
470	.665	.0588
480	.650	.0605
490	.639	.0600
500	.630	.0648

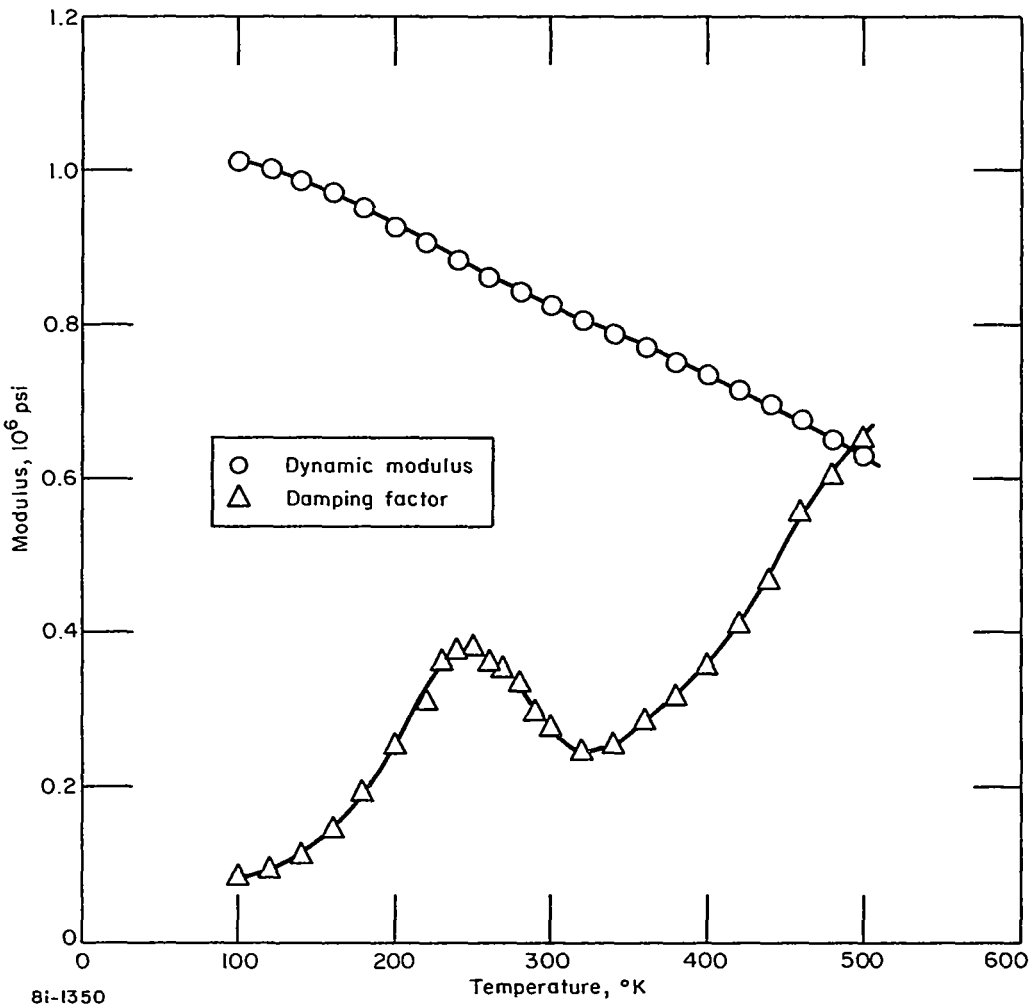

Figure 24 DYNAMIC MODULUS AND DAMPING FACTOR OF POLYIMIDE B

TABLE 10

RELAXATION MODULUS AND SHIFT FACTOR OF POLYIMIDE B

Temperature, °K	Relaxation Modulus At-			Log (1/K)
	1 Sec, 10^6 psi	10 Sec, 10^6 psi	100 Sec, 10^6 psi	
350	.615	.596	.578	-8.0
400	.543	.523	.501	-4.0
450	.501	.485	.466	-2.1
500	.465	.448	.424	0
520	.453	.431	.401	1.0
540	.415	.388	.349	2.2
560	.372	.339	.296	3.5
580	.321	.283	.233	5.2
600	.252	.216	.167	6.8
620				
640				
660				
680				
700				

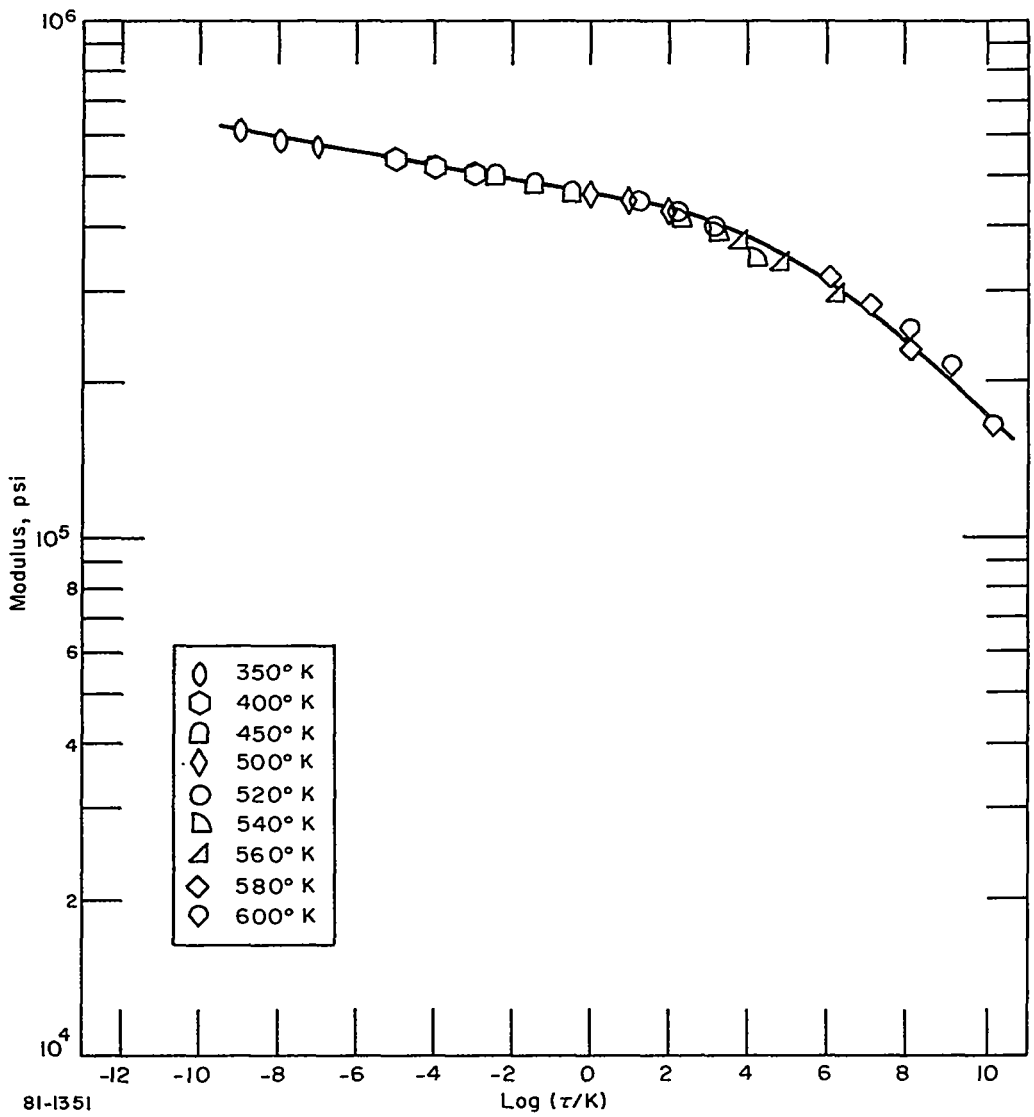

Figure 25 MASTER CURVE OF MODULUS OF POLYIMIDE B

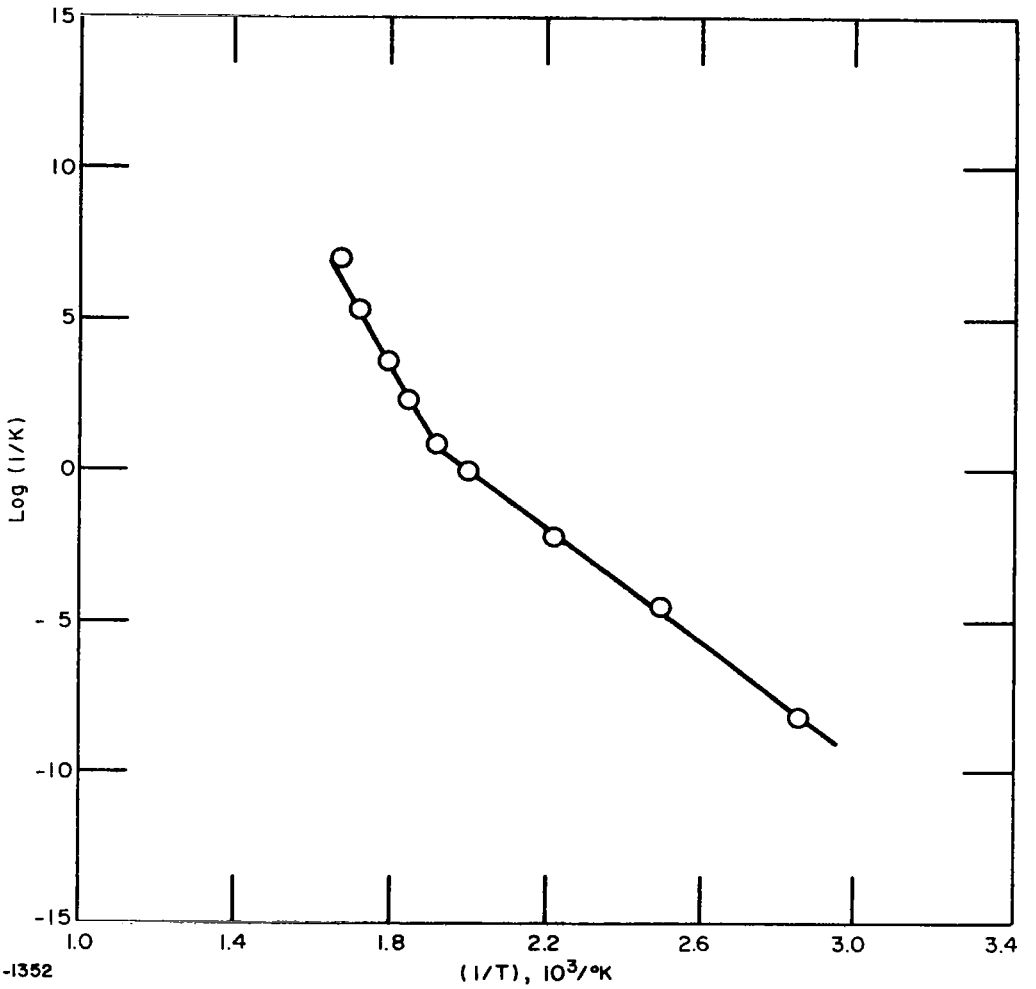

Figure 26 SHIFT FUNCTION OF POLYIMIDE B

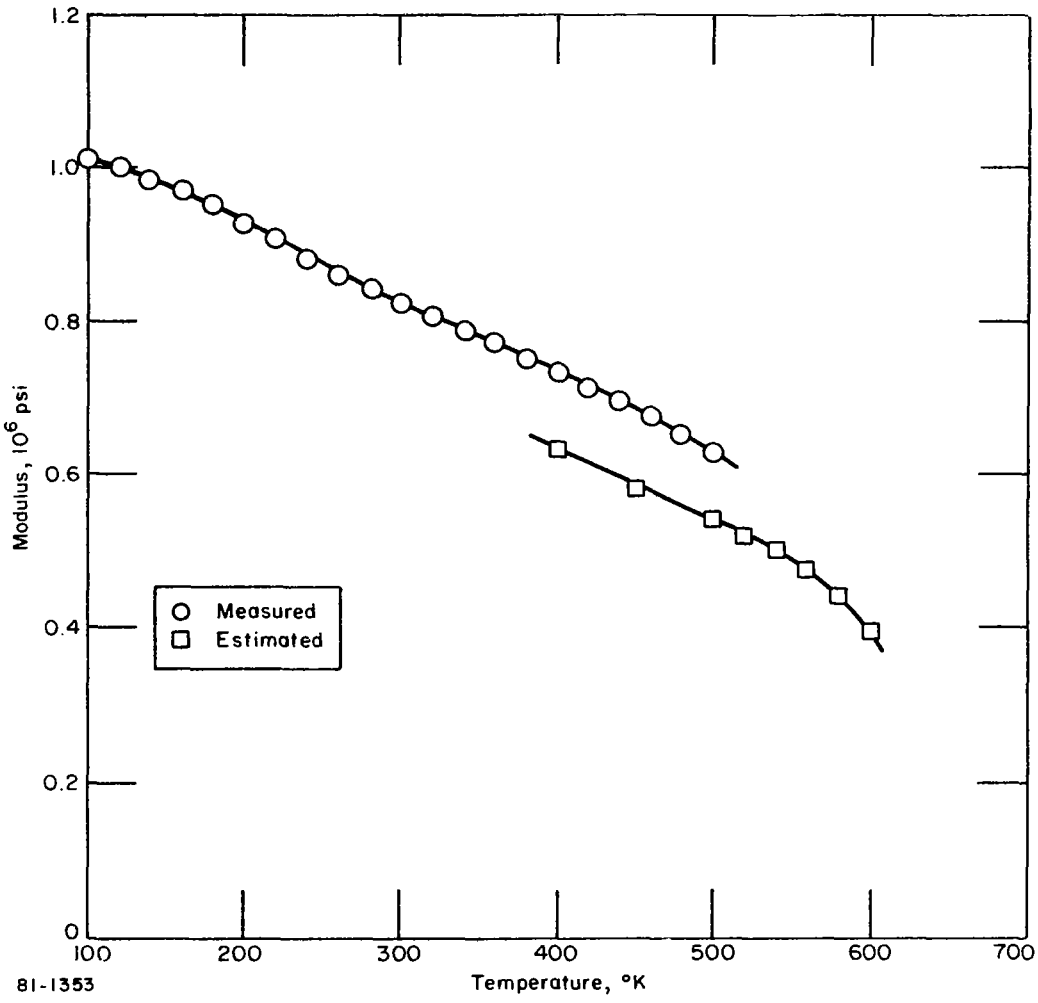

Figure 27 COMPARISON OF ESTIMATED AND MEASURED DYNAMIC MODULI OF POLYIMIDE B

in the specimen holder and more precise machining of the test specimen was incorporated. Any misalignment or non-parallelism in the specimen would impose a lower strain than assumed. This would result in lower calculated relaxation modulus.

The average thermal expansion of seven test specimens is listed in Table 11 and plotted as a function of temperature in Figure 28. The thermal expansion is nearly linear with temperature over the range from 100° to 500°K. Although there are nonlinearities over the 200° to 400°K range, they are sufficiently small that any of several temperatures could be identified (or ignored) as transition temperatures.

Polyimide P.- The average dynamic modulus and damping factors of 24 test specimens are listed in Table 12 and shown as a function of temperature in Figure 29. This material has the lowest modulus of the four polymers and its variation with temperature (in terms of percent change) is greater. The shape of the damping curve in the range from 100° to 300°K is quite similar to that of the other three polymers. As the temperature increases the damping increases, reaching a maximum in the range of 250° to 280°K. Above 300°K, however, the damping curve is quite different, exhibiting two small peaks at about 340° to 410°K.

The average relaxation modulus of 14 test specimens is listed in Table 13. The master curve constructed from these data is shown in Figure 30, and the shift function is shown in Figure 31. If the damping factors at 350°, 400°, and 450°F in Figure 29 are considered, it is seen that they fall essentially on a straight line and hence a transition in the shift function would not be expected. In retrospect, however, it is seen that insufficient stress relaxation data were obtained over the temperature range of 300° to 500°K to resolve the shift function and thereby reflect the transitions observed in the damping curve. There is a break at about 480°K which could correspond to the minimum in the damping curve in this region, and another possible transition at 580°K.

Figure 32 is a comparison between the measured dynamic moduli with those estimated from the master curve. The agreement is good with the two sets falling within 5 percent of each other.

The average expansion of seven test specimens is listed in Table 14 and plotted in Figure 33. Above 200°K the curve of thermal strain versus temperature is non-linear, which is indicative of second order phase changes. The nonlinearities are not large enough, however, to resolve the transitions observed in the damping curve at 340° and 410°K.

TABLE 11

THERMAL STRAIN OF POLYIMIDE B

Temperature, °K	Thermal Strain, %
100	-.575
111	-.547
122	-.515
133	-.489
144	-.456
155	-.427
166	-.400
177	-.369
189	-.335
200	-.305
211	-.276
222	-.241
233	-.210
244	-.177
255	-.145
266	-.111
277	-.074
289	-.038
300	0
311	.044
322	.085
333	.124
344	.169
355	.215
366	.262
377	.311
389	.358
400	.400
411	.446
422	.483
433	.523
444	.560
455	.596
466	.628
477	.659
489	.691
500	.726

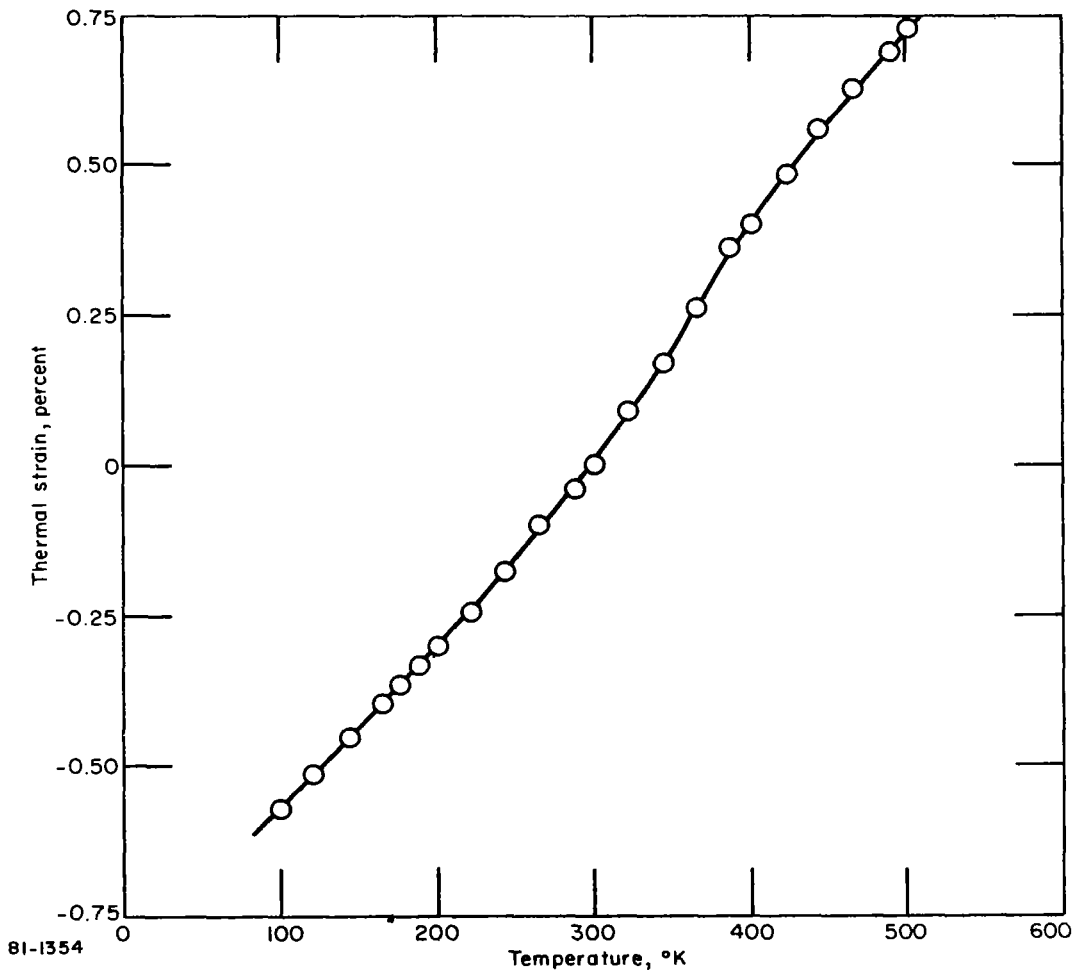

Figure 28 THERMAL STRAIN VERSUS TEMPERATURE OF POLYIMIDE B

TABLE 12

DYNAMIC MODULUS AND DAMPING FACTOR OF POLYIMIDE P

Temperature, ^{o}K	Dynamic Modulus, 10^6 psi	Damping Factor
100	.767	.0205
110	.758	.0196
120	.750	.0201
130	.741	.0206
140	.732	.0215
150	.722	.0215
160	.711	.0225
170	.701	.0245
180	.687	.0265
190	.675	.0306
200	.664	.0354
210	.650	.0409
220	.636	.0445
230	.624	.0520
240	.611	.0559
250	.596	.0573
260	.584	.0574
270	.572	.0577
280	.561	.0553
290	.550	.0541
300	.538	.0503
310	.526	.0480
320	.515	.0480
330	.504	.0479
340	.493	.0486
350	.482	.0486
360	.473	.0479
370	.463	.0456
380	.454	.0446
390	.446	.0442
400	.437	.0463
410	.430	.0468
420	.422	.0428
430	.415	.0415
440	.406	.0401
450	.399	.0402
460	.392	.0383
470	.383	.0367
480	.376	.0386
490	.366	.0376
500	.352	.0403

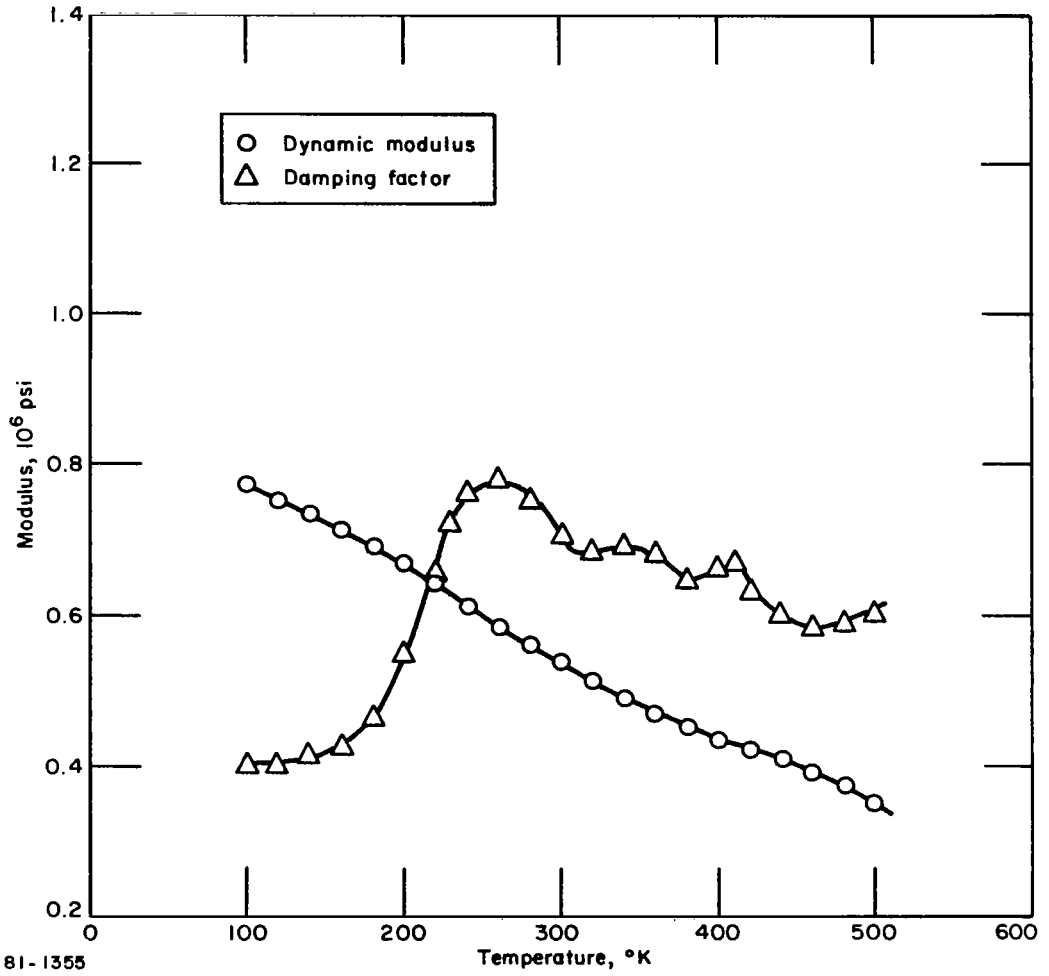

Figure 29 DYNAMIC MODULUS AND DAMPING FACTOR OF POLYIMIDE P

TABLE 13

RELAXATION MODULUS AND SHIFT FACTOR OF POLYIMIDE P

Temperature, ^{o}K	Relaxation Modulus At-			Log (1/K)
	1 Sec, 10^6 psi	10 Sec, 10^6 psi	100 Sec, 10^6 psi	
350	.399	.382	.373	-8.0
400	.365	.353	.341	-4.8
450	.328	.316	.306	-2.3
500	.292	.282	.268	0
520	.281	.269	.252	1.1
540	.262	.251	.234	2.3
560	.253	.240	.224	3.0
580	.233	.220	.200	4.1
600	.216	.203	.182	5.2
620	.197	.184	.165	6.3
640	.179	.162	.147	7.6
660	.156	.145	.127	8.8
680	.136	.124	.127	9.8
700	.116	.104	.089	10.6

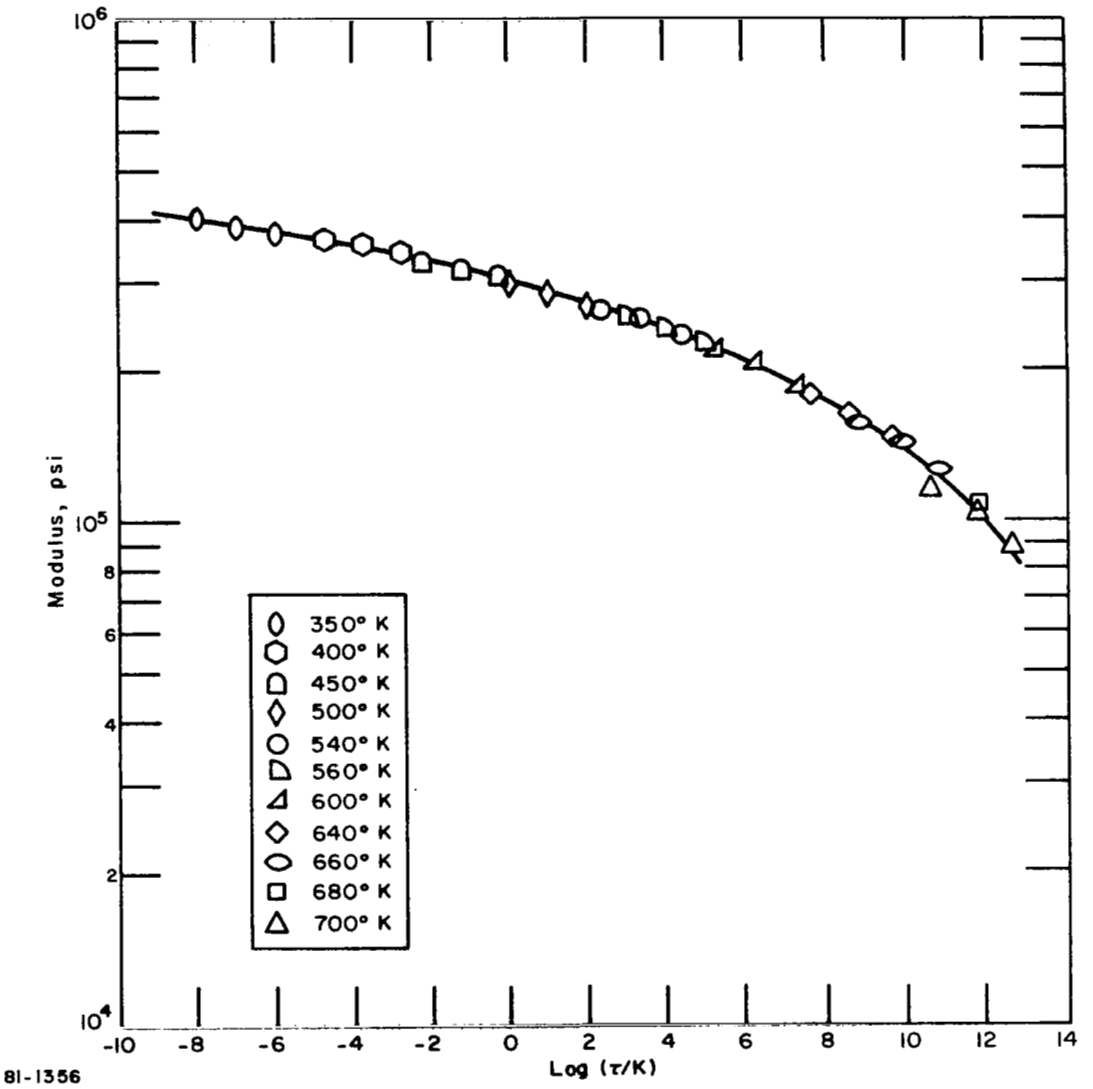

Figure 30 MASTER CURVE OF MODULUS OF POLYIMIDE P

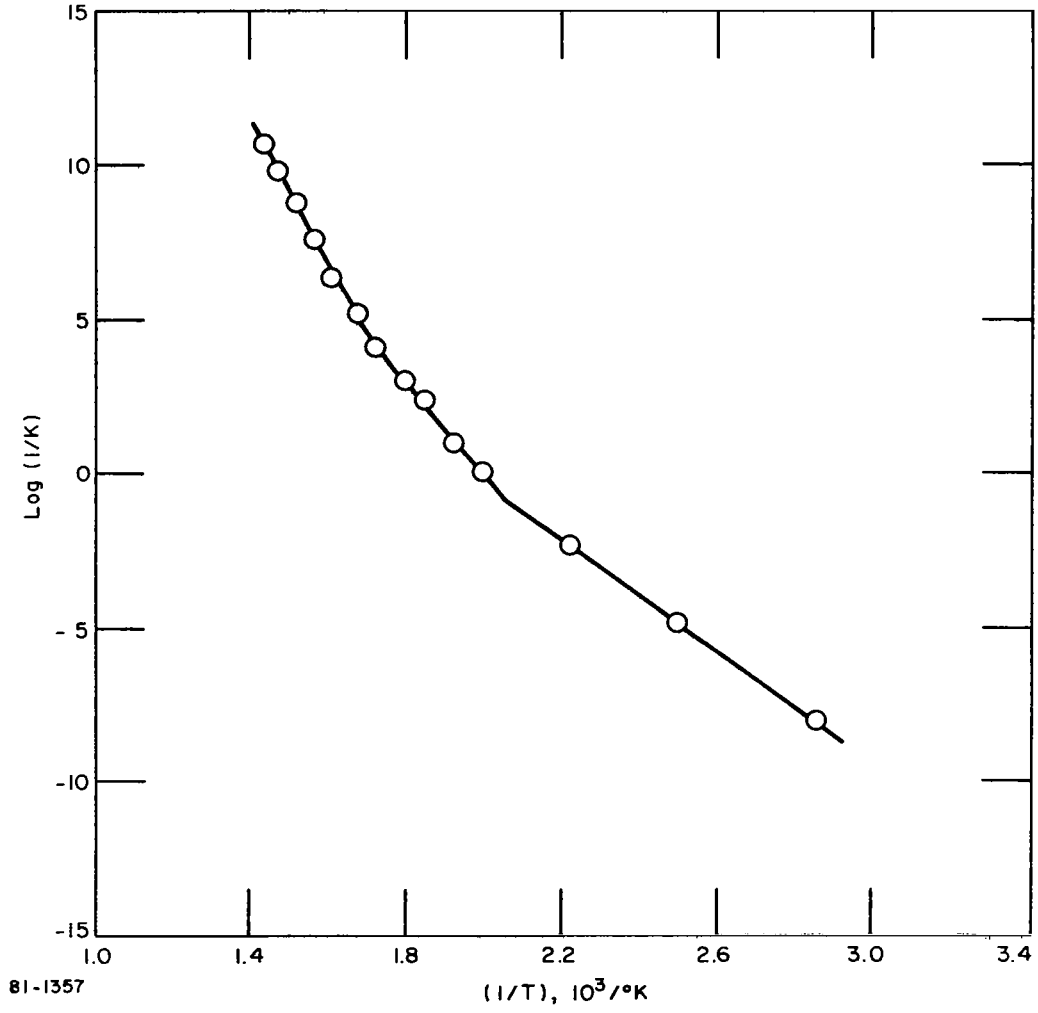

Figure 31 SHIFT FUNCTION OF POLYIMIDE P

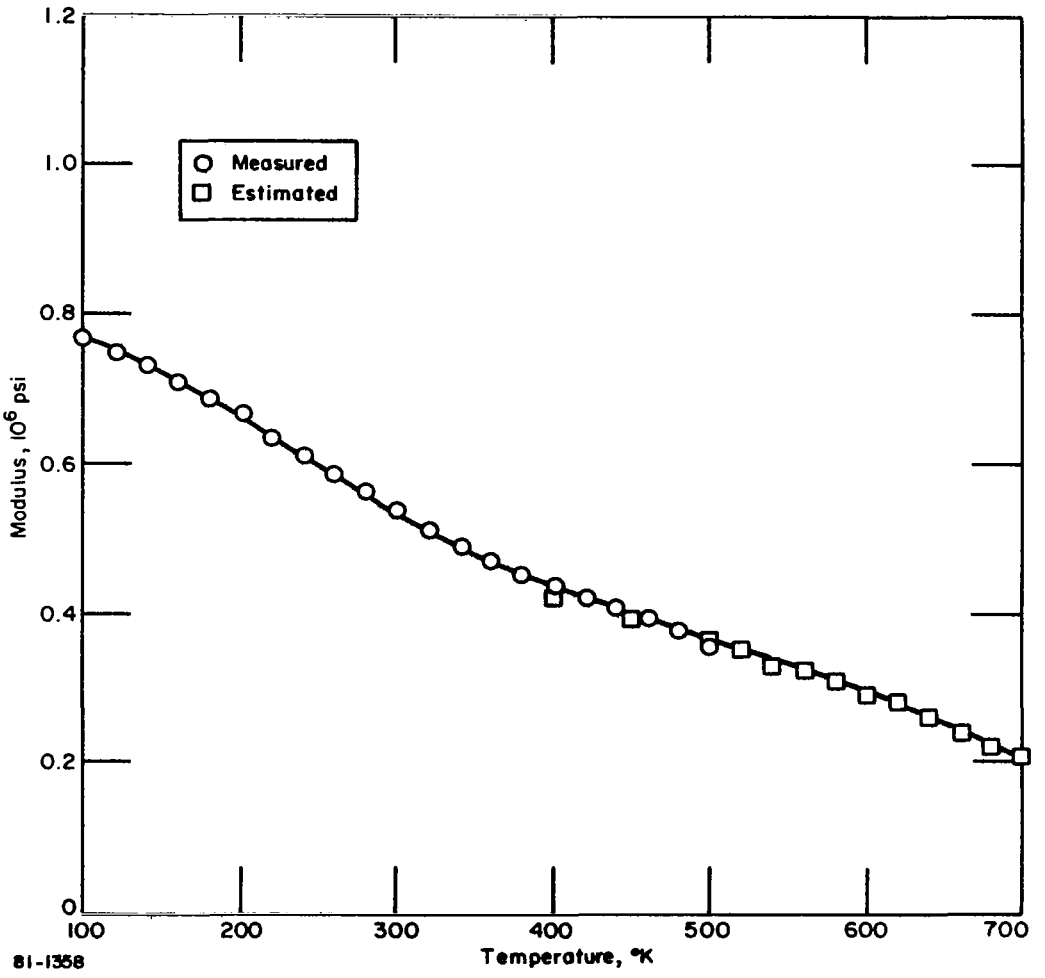

Figure 32 COMPARISON OF ESTIMATED AND MEASURED DYNAMIC MODULI OF POLYIMIDE P

TABLE 14

THERMAL STRAIN OF POLYIMIDE P

Temperature, ^{o}K	Thermal Strain, %
100	-.689
111	-.653
122	-.620
133	-.585
144	-.548
155	-.513
166	-.480
177	-.443
189	-.406
200	-.373
211	-.331
222	-.293
233	-.254
244	-.215
255	-.176
266	-.135
277	-.090
289	-.046
300	0
311	.046
322	.095
333	.144
344	.194
355	.251
366	.308
377	.365
389	.425
400	.478
411	.536
422	.572
433	.652
444	.705
455	.760
466	.821
477	.878
489	.930
500	.980

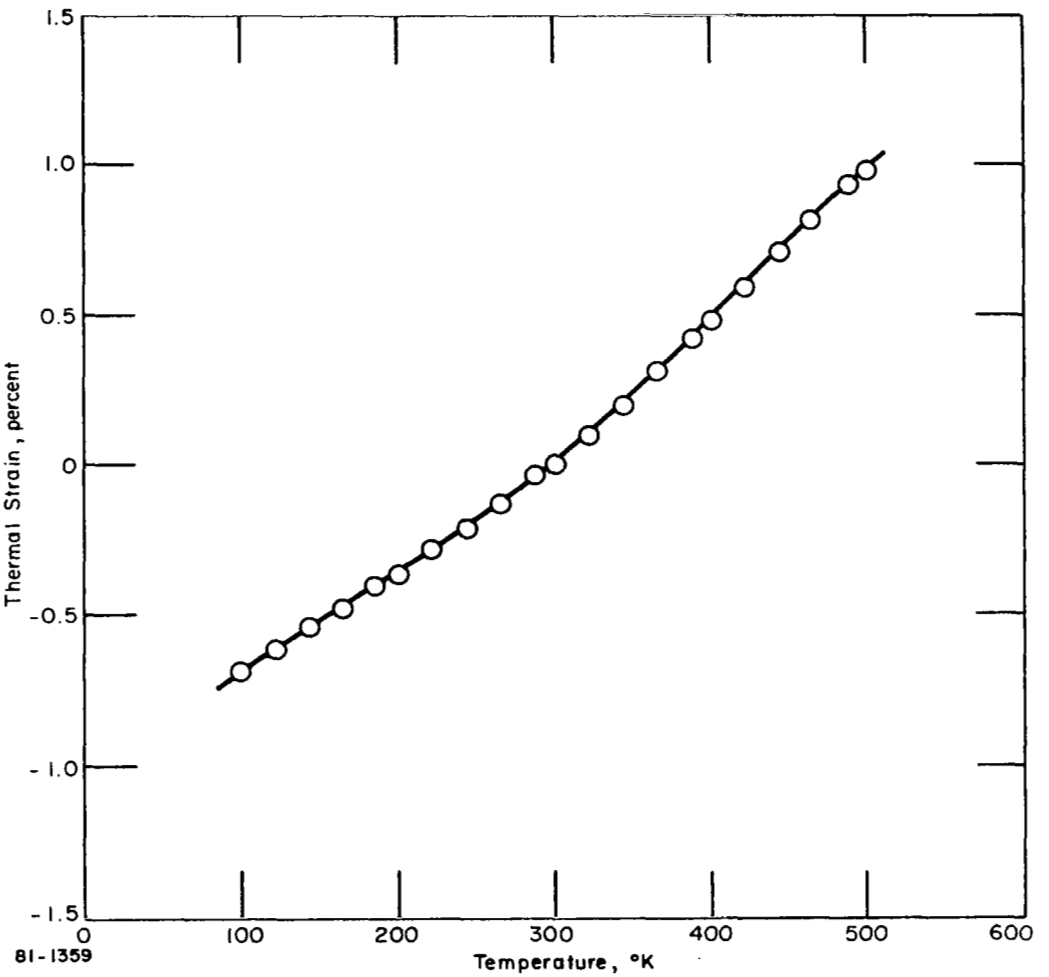

Figure 33 THERMAL STRAIN VERSUS TEMPERATURE OF POLYIMIDE P

CONCLUDING REMARKS

A method has been presented by which the modulus obtained from a long time, low frequency stress relaxation test can be used to estimate the modulus which would be obtained from a short time, high frequency, sonic vibration test. The method is based on the observation that the response of a viscoelastic solid is a function of time and strain only, with no need to incorporate a strain rate term.

The method has been applied to the data obtained on a flexible epoxy which had undergone stress relaxation tests, sonic vibration tests, and high speed stress-strain tests. Despite the wide difference in strain rate, the modulus obtained from the three tests was identical for identical test times. The method was extended to account for the effect of test temperature on the modulus. It was shown that a change in temperature is equivalent to a change in the logarithm of time (time-temperature equivalence), the time and temperature being coupled through a shift function. Furthermore, the change in slope of the shift function-reciprocal temperature curve corresponded to the molecular transition which took place in the epoxy.

An estimate was then made of the dynamic modulus of Pyrrone and polyimide moldings, using stress relaxation modulus data and analyzing the data by means of the time-temperature equivalence method described above. Over the common temperature range (350° to 500°K) in which data from both types of test were available, the estimated dynamic modulus differed by only a few percent from the measured value. The exception was the polyimide B moldings for which the difference in the measured and estimated modulus was approximately 14 percent. The large difference was probably due to extensive cracking of the test specimens and experimental error in the stress relaxation tests. However, in the case of the Pyrrone A, the Pyrrone L, and the polyimide P, the agreement was good enough to conclude that, over the 500° to 700°K range, the estimated dynamic modulus values are accurate.

Langley Research Center,
National Aeronautics and Space Administration,
Hampton, Virginia, July 1971.

-APPENDIX A-

EXPERIMENTAL PROCEDURES

Dynamic Modulus and Damping Tests

Background.- Under this study, the dynamic modulus and damping characteristics were to be determined using a resonant beam. The problem was to select an experimental procedure that (1) could be used over the temperature range from 100° to 700°K, (2) would supply sufficient acoustic energy to overcome the internal damping of these materials, and (3) could be used on specimens of varying geometries. The majority of the specimens had rectangular cross sections (0.50 x 0.12 inch) and were on the order of 3 inches long. Other samples were rods of nominal 0.25-inch diameter and 3.0-inch length. Several experimental approaches were investigated both experimentally and analytically. The experimental approaches used for this study excite the specimen to resonance in a fixed-free mode. Due to transducer limitations the maximum temperature achieved with this approach was 500°K.

Description.- The experimental setup is shown schematically in Figure A1. The major features are (1) a large end mass (~300 grams), (2) a piezoelectric transducer (Kistler Model 912), (3) a specimen mount, (4) the test specimen, and (5) a piezoelectric receiver (Elastomat Model 500).

The mass of the specimen (2 to 4 grams) was small compared to the combined mass of the driver and the end mass (350 grams). Consequently the center of mass of the system is at the driver, thereby making this point a node. The mode of oscillation, therefore, is a fixed-free beam, with the node at the driver-specimen interface and an anti-node at the free end of the specimen.

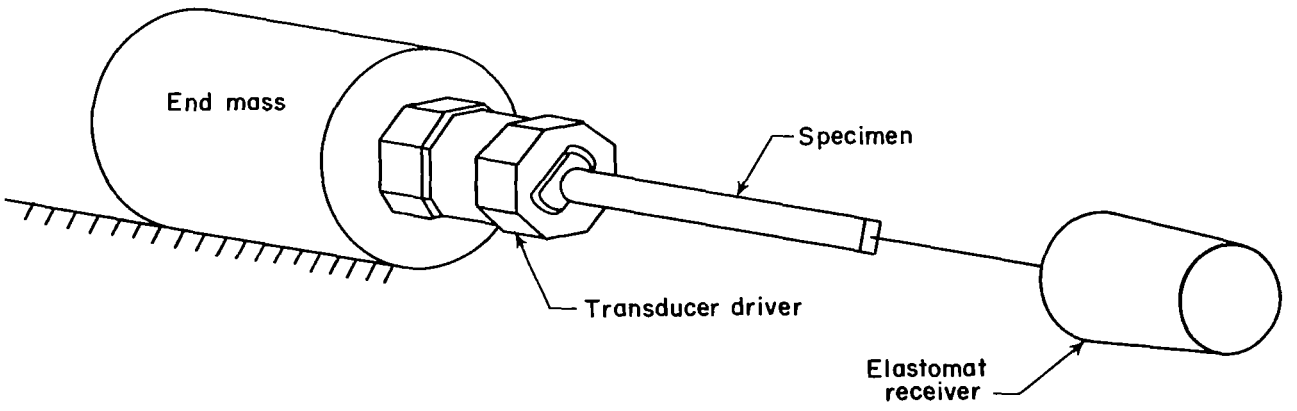

Figure A1 FIXED-FREE ROD EXPERIMENTAL SET-UP

-APPENDIX A-

To ensure that the free end remains an anti-node, the receiver must not load or add an effective mass to the sample. This was accomplished using an Elastomat transducer. This is also a piezoelectric transducer; however, it is coupled to the specimen through a 4-inch long, 0.010-inch diameter quartz fiber. The positions of the node and anti-node were confirmed experimentally by measuring the amplitude of oscillation along the length of the beam.

A signal generator (Hewlett Packard Model 200CD) in conjunction with an audio amplifier (MB Electronics Model 2250) was used to excite the driver. The output of the receiver was fed through the Elastomat for amplification and to determine the frequency. (The Elastomat is equipped with a counter.) The signal was also tapped and fed to an oscilloscope (Tektronic Model RM 565) in order to monitor the magnitude of the received signal.

To attach the specimen to the driver, a threaded button was used. This button had a flat surface to which the specimen was bonded with an epoxy (Baldwin EPY 500 strain gage cement). The threaded portion was used to attach the button-specimen assembly to the driver.

The end mass, driver, and specimen were then placed in a temperature chamber. The environmental chamber used was built by AVCO specifically for thermal expansion measurements and had very good temperature control and gradient (less than $1^{o}K$). The receiver was mounted outside the chamber with the quartz fiber in contact with the specimen through a modified port. The temperature was measured with a thermocouple mounted on the transducer and monitored with a strip chart recorder.

Once the apparatus was at thermal equilibrium the driver was excited and the frequency varied until the fundamental resonant frequency, f_o, was observed. The frequency was then varied on either side of the resonant point to establish the half amplitude frequencies, f_1 (above resonance) and f_2 (below resonance). The dynamic modulus was determined using the relationship:

$$E^* = \frac{KML}{Q} (f_o)^2 . \qquad \text{(A1)}$$

The damping factor was determined using the relationship:

$$\Delta = \left| 1.81 \left(\frac{f_1 - f_2}{f_o} \right) \right| . \qquad \text{(A2)}$$

The calibration run was made on an aluminum sample to establish that the system was providing correct values for a material of known modulus, and to establish the magnitude of the internal damping of the system. The damping of aluminum is on the order of 0.001 to 0.002. Any measured values in excess of this amount could then be considered as the internal damping in the system.

-APPENDIX A-

The data obtained on the aluminum reference sample in the fixed-free mode is listed in Table A1 and plotted as a function of temperature in Figure A2. As will be noted the damping in the range from 100° to 450°K ranges from 0.002 to 0.005 which is within 0.002 of the reported value for aluminum. The internal damping of the system in this range, therefore, is apparently on the order of 0.002 and was considered negligible. From 450°K to 500°K, the measured damping increases to a value of 0.012. No comparable data on aluminum in this temperature range was found and hence one can not tell if this increase is internal to the system or a characteristic of the aluminum. If the damping of the aluminum remains constant at a value of 0.002, the damping of the system would be on the order of 0.010 at 500°K which is on the order of 15 percent of the values measured on the moldings in this range. Based on these data, damping of the system can be considered small in the range from 100° to 450°K and no correction factor need be applied. From 450° to 500°K the damping contribution of the system is unknown and may be as high as 15 percent.

Stress Relaxation Tests

Background.- In a stress relaxation experiment it is necessary to record stress as a function of time while the specimen is maintained at a constant strain. The most difficult part of the experiment is to ensure that the boundary conditions in fact maintain the specimen at constant strain. For this reason, these tests were run in compression. These tests were performed in an Instron Universal Tester (Model TTC) modified by AVCO for performing stress relaxation experiments.

Description.- The stress relaxation apparatus is shown schematically in Figure A3. The major components are (1) load cell on fixed cross head, (2) the specimen and specimen holder, (3) the loading column, (4) a temperature chamber, (5) dead weights, and (6) a micrometer adjustment and stop collar. The key to the system is the micrometer adjustment and stop collar which makes possible a predetermined load train displacement and, hence, a predetermined strain.

The loading column, anvil, and head cell are very rigid. However, they do deform under load and if this deformation is not accounted for, errors as high as 10 percent in the assumed deformation in the sample could occur. The first step in the setup of this experiment, then, is to establish a spring constant for the load train. This is accomplished by removing the specimen and specimen holder and establishing the relationship between the micrometer readings and the applied load.

To begin a test, the movable cross head is raised, lifting the loading column, and a specimen is positioned. With the micrometer set to the zero position, the movable cross head is lowered until it just makes contact with the test specimen (less than 1 percent of the anticipated test load). The

-APPENDIX A-

TABLE A1

DYNAMIC MODULUS AND DAMPING FACTOR OF ALUMINUM REFERENCE SAMPLE

Temperature, ^{o}K	Damping Factor	$EX10^{-6}$ psi	Temperature, ^{o}K	Damping Factor	$Ex10^{-6}$ psi
100	.0046	10.63	310	.0021	9.70
110	.0032	10.61	320	.0021	9.65
120	.0023	10.58	330	.0015	9.60
130	.0029	10.56	340	.0018	9.54
140	.0032	10.53	350	.0018	9.49
150	.0029	10.49	360	.0021	9.43
160	.0026	10.42	370	.0018	9.37
170	.0023	10.39	380	.0021	9.30
180	.0023	10.34	390	.0025	9.22
190	.0020	10.30	400	.0031	9.14
200	.0023	10.25	410	.0040	9.07
210	.0021	10.21	420	.0043	9.01
220	.0021	10.15	430	.0034	8.94
230	.0024	10.10	440	.0038	8.87
240	.0027	10.05	450	.0041	8.81
250	.0033	10.01	460	.0045	8.75
260	.0033	9.96	470	.0051	8.70
270	.0021	9.91	480	.0064	8.61
280	.0024	9.86	490	.0094	8.54
290	.0021	9.81	495	.0097	8.50
300	.0021	9.75	500	.0120	8.45

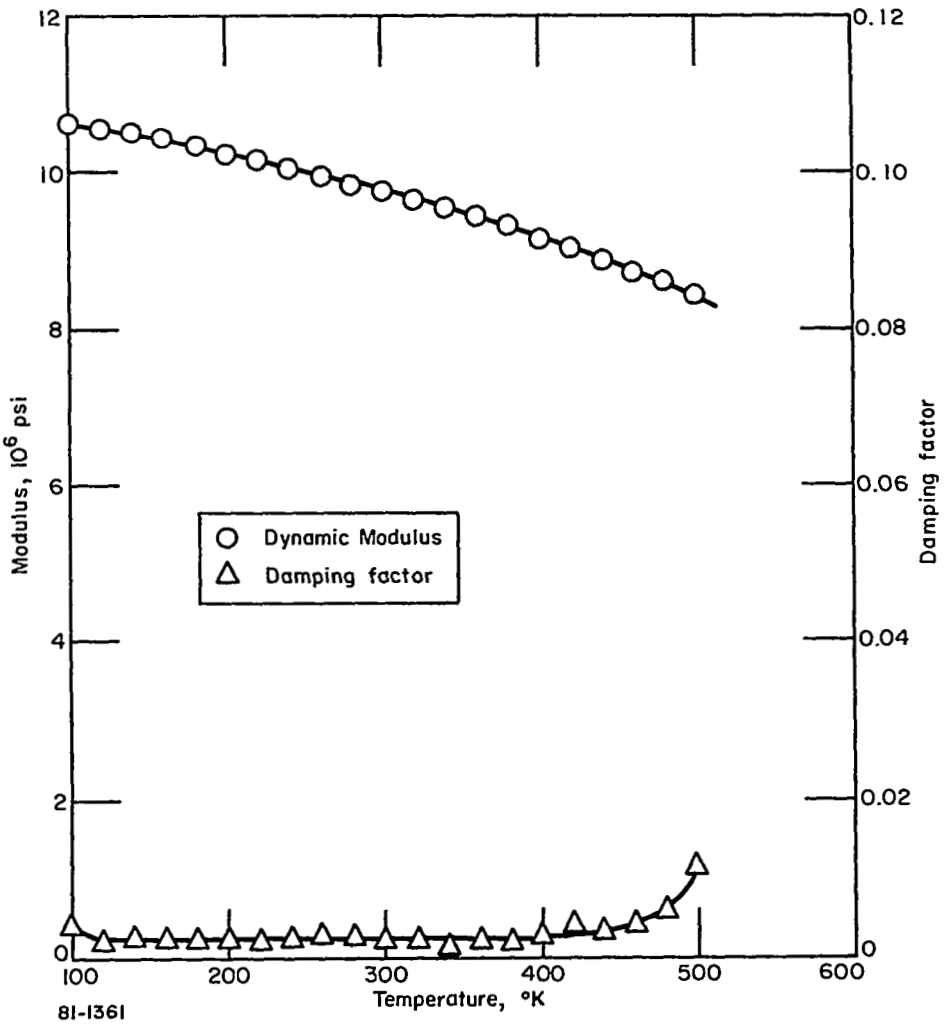

Figure A2 DYNAMIC MODULUS AND DAMPING FACTOR OF ALUMINUM REFERENCE SAMPLE

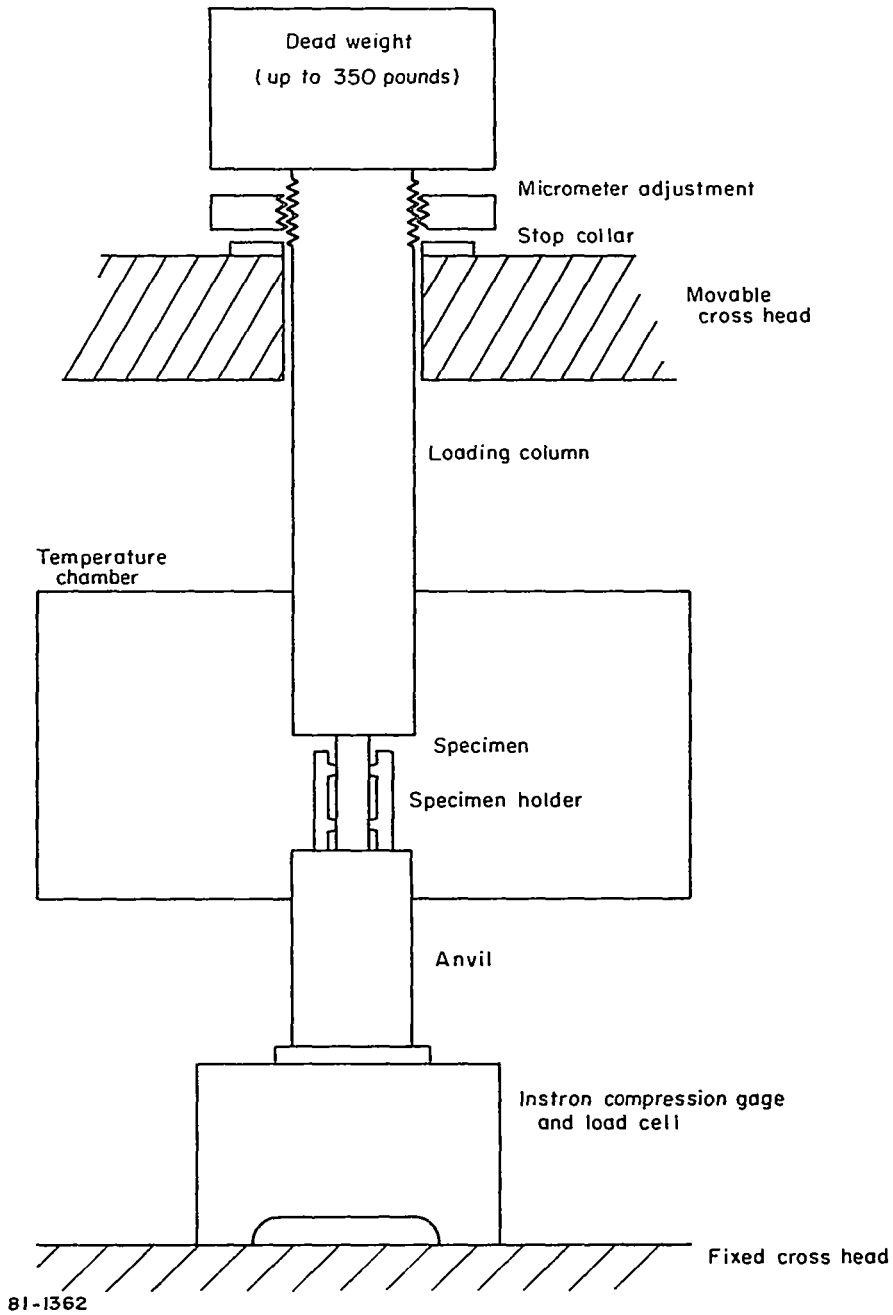

Figure A3 SCHEMATIC OF STRESS RELAXATION APPARATUS

movable cross head will now remain fixed during the remainder of the experiment. The loading column along with the dead weight is then manually lifted so that the micrometer adjustment can be made to produce the desired deflection in the specimen. A ten-to-one lever arm (not shown) is used to lift the column. The weight of the loading column is chosen to exceed that which is required to deform the sample the desired amount. Hence, the loading column will stop when the micrometer adjustment meets the stop collar. The only load sensed by the load cell is that seen by the test specimen.

The loading column is lowered in a period ranging from 0.1 to 0.5 second. The recorder on the Instron has a 1/4-second full-scale response. Reliable data can then be obtained 1 second after the first indication of loading. In this study, the stress at 1, 10, and 100 seconds were recorded. The chart speed on the Instron recorder was 10 in./min.

Thermal Expansion Tests

Thermal strain tests are conducted on an AVCO Corporation built quartz tube dilatometer. The unit consists of a high purity quartz tube inserted in a circulating air environmental chamber in the horizontal position (see Figure A4). An opening in the quartz tube allows the samples (up to 5 inches in length) to be positioned and thermocouples attached, with the output of the thermocouples being fed to a multiprint recorder.

A quartz rod, of quality equal to the tube, is butted against the sample and extended to the open end of the tube where any relative motion between the rod is detected by a linear variable differential transducer. The output of the transducer is fed to the same recorder as the temperature, thereby providing a record of temperature and strain versus time.

The temperature control is provided by an AVCO built temperature controller. This controller is capable of temperature step control but is normally operated on the automatic programming mode which yields precise and continuous increase of temperature at a rate of $1.1^{o}K$ per minute.

The thermal expansion characteristics are presented in this report as differential strain with respect to $300^{o}K$. These values have been corrected for the expansion of the quartz.

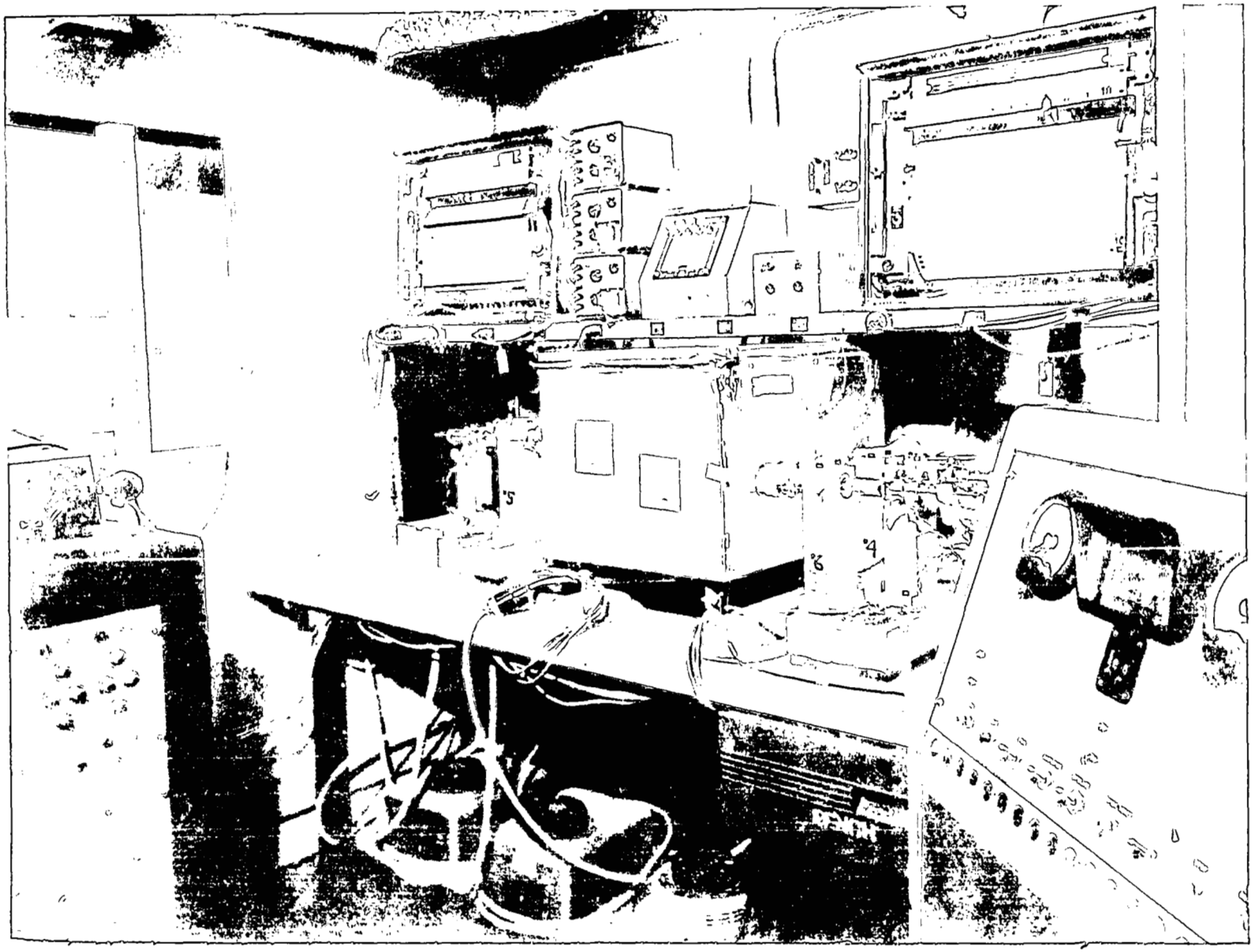

Figure A4 THERMAL EXPANSION APPARATUS

-APPENDIX B-

CURVE FITTING TECHNIQUE

Introduction

Often it is difficult to envision the mechanics involved in fitting a set of data to a time-temperature superposition. The following is a brief step by step description of a curve fitting technique which was used in the treatment of the data generated in this program. The data used as an illustration is that obtained on the Pyrrone A and is listed in Table 1.

Discussion

There is an old adage that one can prove any point by plotting the data on a log-log scale. While it is not necessary to use a log-log scale to arrive at a time-temperature superposition it is necessary to use the logarithm of time and often a clearer picture is obtained by using the logarithm of stress or modulus also. This is the approach taken here.

Starting with the modulus data of various times and temperatures (see Table 1) determine the values of Log E and Log τ (See Table B1). It is, of course, not necessary to determine the logarithm of each value; the data could be plotted on logarithmic or semi-logarithmic axes. The next step is to plot the Log E* versus Log τ at each temperature (See Figure B1). Only four temperatures have been included for simplicity. These curves may now be shifted along the Log τ scale to establish a master curve of modulus E* versus the parameter Log τ/K where τ is time and (1/K) is a temperature dependent parameter. This master curve is constructed by plotting the curve at each temperature on a separate piece of paper. Then with the use of a light box, the curve for the reference temperature is placed in some arbitrary position. The choice of reference temperature is arbitrary and was chosen at 500° K for this study.

The 560°K curve is then positioned on top of the 500°K curve so that the Log E* scales are aligned. The 560°K curve is then shifted towards the right until the two sets of data overlap. When working with a logarithmic scale this shifting is in essence multiplying the entire 560°K time scale by a constant (1/K). The value of Log (1/K) is established by determining the number of units on the Log τ scale that the curve was shifted towards the right side in order that the two curves overlap. In the illustration used here, the 560°K curve must be moved 1.0 units along the time scale for the 500° and 560°K curves to overlap (see Figure B2). The value of log (1/K) at 560° K is then 1.0.

With the 500° and 560°K curves kept in the same relative position, the 580°K curve is then placed on top, again with Log E* scales aligned. The 580°K curve is then shifted until it overlaps the previous curves. The amount the 580°K curve had to be shifted (with respect to the reference 500°K

-APPENDIX B-

TABLE B1

LOGARITHM OF RELAXATION MODULUS OF PYRRONE A

Temperature, ^{o}K	Log Relaxation Modulus at-		
	1 sec	10 sec	100 sec
160	6.045	6.037	6.017
180	6.029	6.025	6.009
200	6.021	6.017	6.000
220	6.017	6.013	6.000
240	6.004	6.004	5.987
260	6.000	5.991	5.982
280	5.987	5.978	5.964
300	5.978	5.968	5.954
320	5.954	5.944	5.934
340	5.944	5.924	5.903
360	5.908	5.881	5.845
380	5.886	5.851	5.813
400	5.845	5.806	5.763
450	5.778	5.732	5.672
500	5.716	5.662	5.580
520	5.700	5.653	5.568
540	5.680	5.683	5.531
560	5.653	5.602	5.491
580	5.591	5.519	5.362
600	5.505	5.431	5.255
620	5.452	5.362	5.204
640	5.415	5.322	5.176
660	5.415	5.342	5.204
680	5.398	5.322	5.176
700	5.322	5.230	5.041

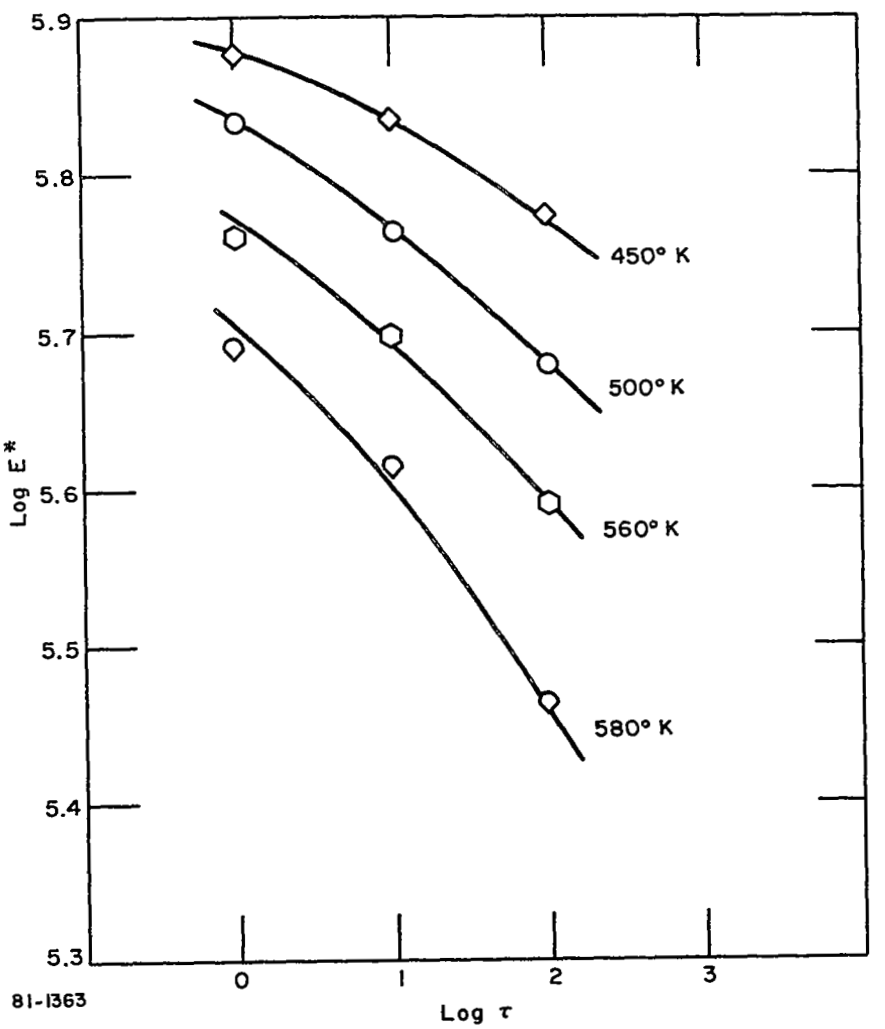

Figure B1 MODULUS VERSUS TIME AT VARIOUS TEMPERATURES OF PYRRONE A

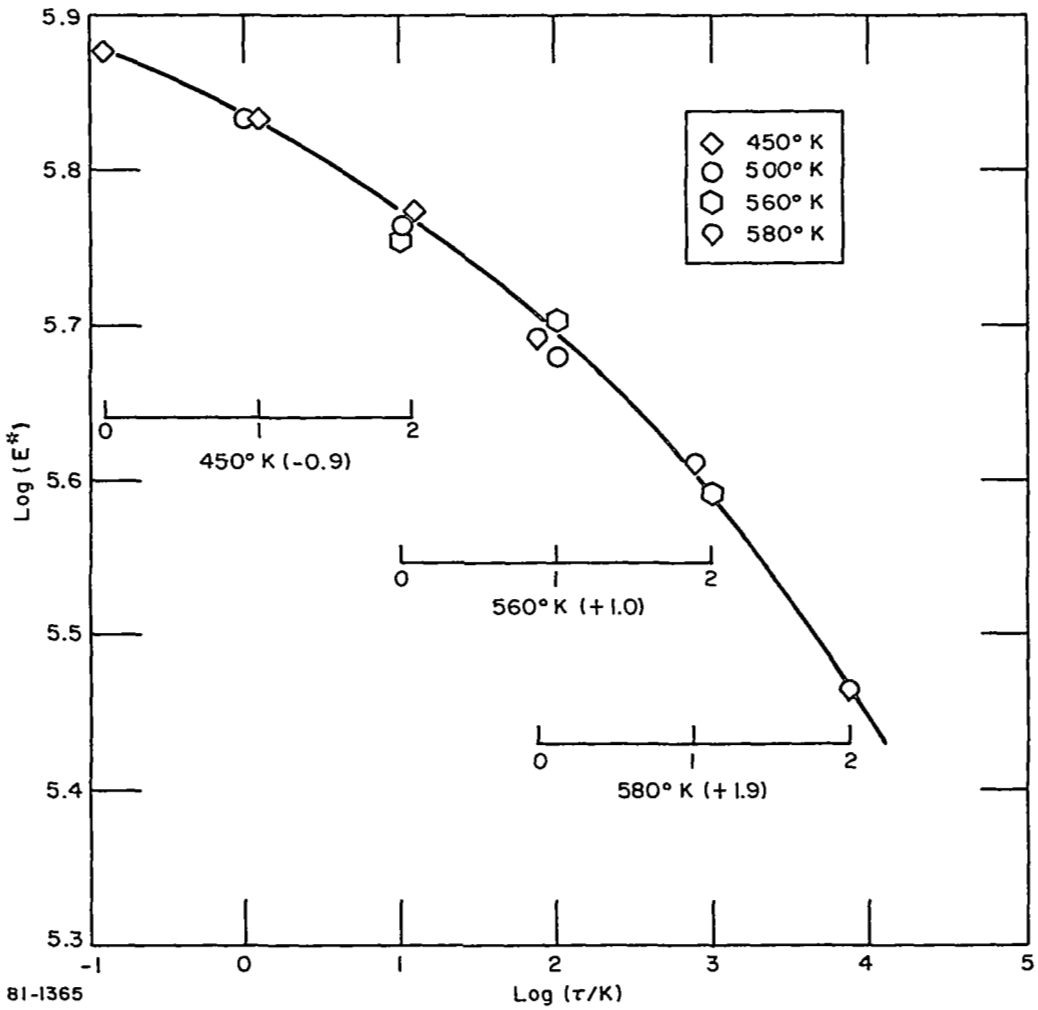

Figure B2 MASTER CURVE OF MODULUS OF PYRRONE A

curve) was 1.9 units on the Log τ scale (see Figure B2). The value of Log (1/K) at 580°K is then 1.9. This same process is followed for all the curves at temperatures above 580°K. The value of Log (1/K) for each temperature is then the number of units each curve had to be shifted towards the right so that the curves would superimpose over the reference temperature curve.

For those curves at temperatures below the 500°K reference temperature the shift must be towards the left. In order for the 450°K data to superimpose or overlap, the curve had to be shifted 0.9 units towards the left. The value of Log (1/K) is then -0.9. Again the same process is followed for those curves below the reference temperature and the values of Log (1/K) will be negative.

The next step is to establish how the shift function (Log 1/K) varies with temperature. For materials which do not undergo a phase change in the temperature range of interest, there is considerable justification to expect that the shift function will follow an Arrhenius type of activation. In other words, the shift function will be of the form:

$$(1/K) = Ae^{-B/T}.$$

Therefore, a plot of Log (1/K) versus the reciprocal of absolute temperature should be linear, with a slope of B and an intercept of A. If a phase change occurs within the temperature range of interest, one would expect a plot of Log (1/K) versus the reciprocal of absolute temperature would depart from linearity and exhibit a different slope or activation energy for the different phases.

For the data used as an illustration here, the finished master curve is shown in Figure 12 and the shift function established is shown in Figure 13.

REFERENCES

1. Hughes, C.T.: Preparation and Characterization of Low DP End-Capped Pyrrone Moldings. NASA CR-1633, August 1970.

2. Bell, Vernon L.: Heteroaromatic Polymers via Salt Intermediates. Polymer Letters, Vol. 5, pp. 941-946, 1967.

3. Price, Howard L.; and Bell, Vernon L.: Preparation and Compression Molding of Salt-Like Intermediate Pyrrone (BTDA-EG-DAB). Presented at 27th Annual Technical Conference, Society of Plastics Engineers (Chicago, Illinois), May 5-9, 1969.

4. Hilton, Harry H.: Viscoelastic Analysis. Chapter 4 Engineering Design for Plastics, Eric Baer, ed., Reinhold Publishing Corporation, 1964.

5. Lander, Louis: A discussion on the Equivalence of Stress Relaxation Modulus and Various Dynamic Modulus Data. Presented at the 73rd Annual Meeting of the American Society for Testing and Materials (Toronto, Canada), 21-26 June 1970.

6. Schwarzl, F.; and Staverman, A. J.: Time-Temperature Dependence of Linear Viscoelastic Behavior. Journal Applied Physics, Vol. 23, No. 8 August 1952.

7. Takayanagi, Motowo: Viscoelastic Behavior of Crystalline Polymers. Proceedings Fourth International Congress on Rheology, August 26-30, 1963, Part 1. Interscience Publishers, 1965.

NASA-Langley, 1972 —— 18 CR-1946